Selection and hybridization shaped the Africanized honey bee invasion of the Americas

Erin Calfee[1*], Marcelo Nicolás Agra[2], María Alejandra Palacio[2], Santiago R. Ramírez[1], Graham Coop[1]

1 Department of Evolution and Ecology & Center for Population Biology, University of California, Davis
2 National Institute of Agricultural Technology (INTA), Balcarce, Argentina

*** ecalfee@ucdavis.edu**

Abstract

Recent biological invasions offer remarkable 'natural' laboratories to understand the genetics and ecology of adaptation, hybridization, and range limits. One of the most impressive and well-documented invasions of the 20th century began in Brazil with the escape of introduced African honey bees (*Apis mellifera scutellata*) in 1957. In less than 50 years, populations of 'Africanized' honey bees spread across much of the Americas, hybridizing with and outcompeting resident European honey bees. We use broad geographic sampling and whole genome sequencing of over 300 bees to map the distribution of African ancestry where the northern and southern invasions have presently stalled, forming replicated hybrid zones between Africanized and European bees in California and Argentina. California is much further from Brazil, yet these hybrid zones occur at very similar latitudes, consistent with the invasion having reached a climate barrier. At these range limits, we observe genome-wide clines for African ancestry, and parallel clines for wing length that span hundreds of kilometers, supporting a smooth transition from climates favoring Africanized bees to climates where they cannot survive winter. Ancestry clines at individual SNPs are consistent with a broad genetic basis for climate-associated fitness trade-offs, with a build-up of somewhat steeper clines in regions of low recombination and no large effect loci maintaining exceptionally steep ancestry transitions. Additionally, we find no substantial reductions in genetic diversity associated with rapid expansions nor complete dropout of African ancestry at any individual loci, which suggests that the competitive fitness advantage of African ancestry at lower latitudes has a broad genetic basis and that Africanized bees maintained large population sizes during their invasion. To test for parallel selection across continents, we develop a null model that accounts for drift in ancestry frequencies during the rapid expansion. We identify several peaks within a larger genomic region where selection has pushed African ancestry to high frequency hundreds of kilometers past the present cline centers in both North and South America and that may underlie high-fitness African traits driving the invasion.

Introduction

Diverging lineages often spread back into secondary contact before reproductive isolation is complete, and so can hybridize. In hybrid zones, multiple generations of

admixture and backcrossing create a natural experiment in which genetic variation is 'tested' in novel ecological and genomic contexts. The mosaic of ancestries in hybrid zones has allowed researchers to uncover the genetic loci associated with reproductive barriers (e.g. [71, 74]) and to identify rapidly introgressing high-fitness alleles (e.g. [24, 34, 36]). One promising way forward is to compare ancestry patterns across multiple young hybrid zones and test how repeatable the outcome of hybridization is across these evolutionary replicates.

In this study, we use this powerful comparative framework to better understand the genomic basis of fitness and range limits in the Africanized honey bee invasion, with replicate hybrid zones in North and South America. In 1957, newly introduced honey bees of African ancestry (*Apis mellifera scutellata*) escaped from an experimental breeding program in Brazil and rapidly dispersed. Invading African bees both out-competed and hybridized with European-ancestry populations, creating a rapidly advancing admixed population of 'Africanized' bees that expanded north and south across the Americas at 300-500 km/year [84].

The highly defensive behavior of Africanized honey bees, and the implications for commercial bee management and public health, sparked immediate international concern over the outcome of this invasion. Control efforts have been largely unsuccessful in preventing Africanized honey bees from permeating feral and commercial colonies within their expanding range [84]. However, even without intervention, Africanized honey bees are unlikely to outcompete European bees in the coldest regions of the Americas because of their low overwinter survival in climates where European bees thrive [79, 85]. Models based on winter temperatures and the physiological cost of thermo-regulation predict northern range limits that vary from the Central Californian Coast [31, 73] up to the border with Canada [66]. Thus, the expected impact of Africanized honey bees on agriculture and queen bee production in the United States is still poorly defined. Broad surveys show that African mtDNA and Africanized phenotypes are common in northern Argentina and the southern US, and drop off towards more temperate latitudes, indicating that the rapid spread of these traits has dramatically slowed, if not stopped, on both continents [2, 43, 46, 48, 57, 62, 73]. However, we lack a genome-wide view of the range limits of Africanized ancestry and do not know whether individual high-fitness alleles have already introgressed into higher latitudes.

A number of studies have corroborated the historical record of this trans-American invasion at the genomic level, showing that honey bees in the Americas are historically admixed between predominately eastern European (C) and western European (M) subspecies, while the recently introduced Africanized honey bees are predominantly a genetic mixture of African (A) and European C & M subspecies [9, 13, 41, 81, 83]. A recent study of Africanized bees in Brazil revealed some European alleles at exceptionally high frequency that may have contributed to the success of the invasion, but this work was under-powered to detect high-fitness African alleles due to elevated genome-wide African ancestry (84%) in the Brazilian population [54].

While the key genes remain unknown, bees with African ancestry diverge from European-ancestry bees on a number of traits that may have given Africanized honey bees a selective advantage during the invasion: they defend their colonies more aggressively [37, 38], they have higher reproductive rates (including faster development times, proportionally higher investment in drone production and more frequent swarming to found new colonies [84]), they have higher tolerances to several common pesticides [20], and they prove less susceptible to *Varroa* mites, a major parasite [28, 29, 50, 53, 78]. Population monitoring studies show that *Varroa* mites are a strong selective force in the wild and that mite infestations in the 1990s likely contributed to the rapid genetic turnover of feral nest sites from European to Africanized colonies in Arizona and Texas [9, 48, 57].

There are also a number of candidate traits that differ between African and European bees and plausibly contribute to a climate-based range limit for the invasion. Smaller bodies [17] and higher metabolic rates [66], for example, could give Africanized honey bees a competitive advantage in the tropics but come at a cost in cooler climates [31]. In addition to physiological traits, heritable behaviors may also contribute to fitness trade-offs: African ancestry bees preferentially forage for protein-rich pollen (vs. nectar), which supports rapid brood production, but risks insufficient honey stores to thermo-regulate over winter [19, 23, 31].

Here we conduct the first comparative study of the Africanized honey bee invasion in North and South America. First, we use broad geographic sampling and whole genome sequencing to map the present-day ancestry clines on both continents, and assess the evidence for a climatic barrier preventing the further spread of Africanized honey bees. Next, we use genetic diversity within African ancestry to study the shared bottleneck within and amongst populations due to the rapid expansion during the invasion. Finally, we develop a null model that includes recent drift and use this model to test for outlier loci that may underlie high-fitness African traits and climatic barriers.

Results

To survey the current geographic distribution of African ancestry in the Americas, we sampled and sequenced freely foraging honey bees across two latitudinal transects, one in California and one in Argentina, formed from the northern and southern routes of invasion out of Brazil (see Fig 1). We generated individual low-coverage whole-genome sequence data for 278 bees, and added to this data set 35 recently published high-coverage bee genomes from 6 additional California populations sampled 3-4 years prior [13]. We inferred genome-wide ancestry proportions for each individual using NGSAdmix [65] assuming a model of 3 mixing populations, which clearly map to the African (A), eastern European (C), and western European (M) reference panels (see Figs 1 and 2). We leveraged the fact that admixed Africanized honey bee populations were formed through a recent mixture of well-defined honey bee subspecies to infer the mosaic of African (A) and European (C & M) ancestry tracts across the genome of each bee using a hidden Markov model (ancestry_hmm [12]). The average local ancestry estimates within individuals agree closely with the NGSAdmix genome-wide ancestry estimates (see Fig 3, Pearson's $r \geq 0.985$), with the HMM estimating slightly higher minor ancestry for low admixture proportions, likely as a result of some miscalled blocks. Time estimates vary by population, with a median of 47.6 generations in the 62 years since the initial dispersal of Africanized bees out of São Paulo (see Fig 5 for all time estimates). In this section, we first focus on the distribution of genome-wide 'global' ancestry patterns across the two clines, which we will later compare to the variation in local ancestry at individual loci.

We observe wide hybrid zones mirrored in North and South America. In Argentina, we find the cline in ancestry spans nearly 900km, from 77% A ancestry in the north to less than 5% to the south in Buenos Aires Province. The current geographic range of Africanized honey bees in South America is broadly consistent with prior studies using a smaller number of genetic markers (e.g. [1, 2, 62, 83]), though the geographic and genetic resolution of these studies is too limited for detailed comparison. In North America, we find that honey bees in California have up to 42% African ancestry in the south, tapering down to approximately 0% in Davis, our northernmost sampling site. In comparison, earlier extrapolations based on mitochondrial surveys may have somewhat overestimated genome-wide African ancestry in California (e.g. 65% of foraging bees in San Diego County [43] and 17% in Monterey County [46] carry African mtDNA haplotypes).

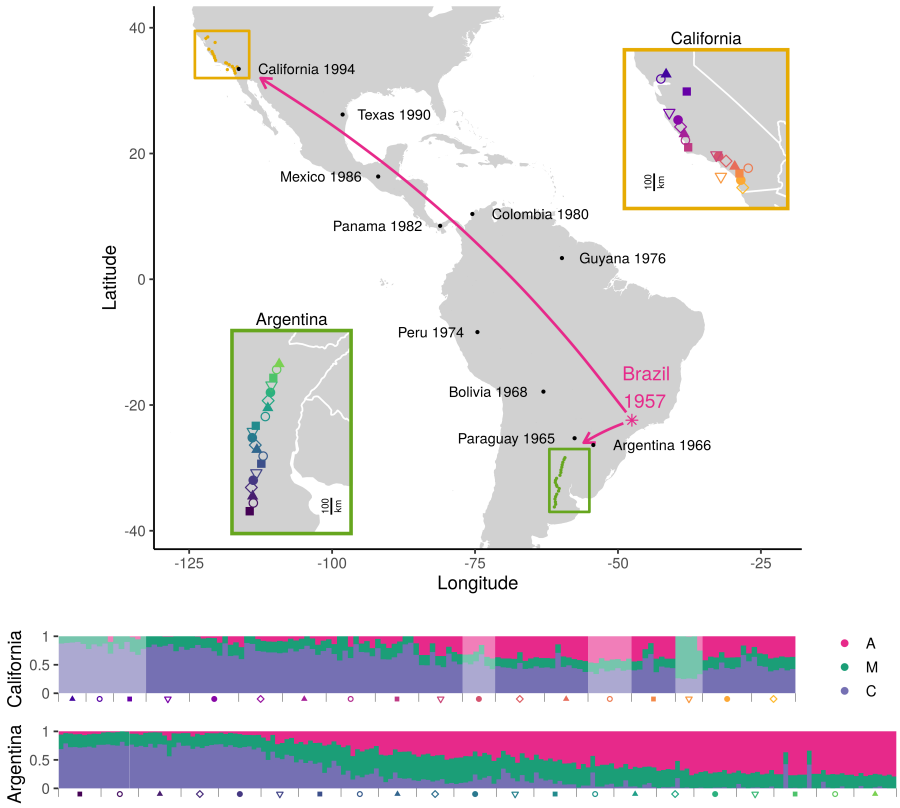

Fig 1. Spread of Africanized honey bees. Map of hybrid zones in California and Argentina, with cartoon arrows depicting the two routes of Africanized honey bee invasion out of Rio Claro, São Paulo, Brazil. Dates of first occurrence along the routes of invasion are from [84] [42] and [77], with approximate GPS locations extracted from google maps. Insets zoom in on each hybrid zone to show the mean GPS coordinates for each sampled population. Genome-wide A, C, and M ancestry inferred using NGSAdmix for each bee are shown in a bar chart at the bottom, where each vertical bar is one bee and colors indicate proportion ancestry. Populations are arranged by latitude, with samples closest to Brazil on the right. Light fading indicates that a bee comes from the previously published California data set [13] and was collected in the field 3-4 years prior to the bees from this study.

Alongside our genomic cline, we find a corresponding phenotypic cline in worker fore wing size: closer to the equator, sampled bees have increasing African ancestry and shorter wings (see Fig 2). By fitting a linear model to predict wing length from genome-wide ancestry, we find that African ancestry can explain a difference of -0.72mm, approximately an 8% reduction in wing length ($P = 3.65 \times 10^{-23}, R^2 = 0.31, n = 269$; see Fig 7). We tested for a main effect and an interaction term for the South American continent, and found no significant differences in wing length ($P = 0.81$) or its association with ancestry ($P = 0.86$) between the two clines. Thus, in contrast to the rise of dispersal-enhancing traits in other recent invasions (e.g. [16, 33, 56, 64]), we see no evidence of a bias for longer wings at larger dispersal distances (California). While we cannot rule out a role for developmental plasticity, since bees were sampled from across a temperature gradient, genetic crosses have shown that wing length differences between ancestries have a genetic basis [38]. We find that and the wing length patterns we observe here are consistent with expectations of an additive polygenic cline based on

genome-wide ancestry alone (see Fig 2). We performed admixture mapping to test for genetic loci underlying ancestry-associated differences in wing length and did not identify any loci meeting genome-wide significance (see Fig 9).

Our genomic results indicate that the geographic distribution of Africanized honey bees is presently constrained by climatic barriers, not dispersal. Historical records document an initial rapid spread of Africanized honey bees from their point of origin in Rio Claro, São Paulo, Brazil, followed by the formation of seemingly stable hybrid zones at similar latitudes in North and South America. Yet to reach this same latitude, northern-spreading bees had to travel more than five times the distance as southern-spreading Africanized honey bees.

To more precisely infer the current shape and position of the two hybrid zones, we fit a classic logistic cline model to observed genome-wide individual African ancestry proportions [69, 70, 82]:

$$A_i = \frac{M}{1 + e^{-b(x_i - c)}}, \tag{1}$$

where A_i is the genome-wide African ancestry proportion inferred for the ith individual bee, x_i is their latitude, M is the asymptotic maximum African ancestry approaching the equator, which is set at 0.84 (i.e. frequency in Brazil [54]), c is the cline center, and $w = |4/b|$ is the cline width. Each degree latitude corresponds to approximately 111km and presents a natural way to compare cline position and shape between the two zones. We fit this model in R using non-linear least squares. We find that the two hybrid zones have strikingly similar positions (see Fig 2), with cline centers that differ by less than half a degree (32.72°N vs. 32.26°S), and no statistically significant difference in cline steepness. To better understand the mechanisms underlying this parallelism between continents, we tested four possible explanatory climate variables to see if we could identify a better predictor for African ancestry across our two zones than latitude: Mean annual temperature (°C), mean temperature of the coldest quarter (°C), minimum temperature of the coldest month (°C), and mean annual precipitation (cm) (downloaded from WorldClim.org [32]). We fit clines for both hybrid zones jointly using these four environmental variables in turn as predictors in Eq 1 in place of x_i, and compared these results to fits based on absolute latitude and, as a neutral dispersal model, distance from São Paulo.

We find that latitude is the best individual predictor of genome-wide global ancestry, and mean annual temperature the second-best predictor, as assessed by AIC (see S2 Table). While latitude provides the best-fitting cline, we find it unlikely that latitude or daylight per se is the relevant selection gradient. Temperature and precipitation are closely coupled to latitude across our transect in Argentina, so nearly all of our resolution to disentangle latitude from environmental gradients comes from micro-climates within California, and for precipitation, the contrast between continents (see Fig 6). However, we failed to identify specific environmental variables that may be driving the relationship with latitude, either because we did not include the relevant environmental variable(s) or because the climate data does not reflect the selection environment of sampled bees, e.g. due to mismatches in scale or selective habitat use by bees within a foraging range.

Despite limited resolution on the climate variables driving the latitudinal gradient, our comparative framework allows us to firmly reject a neutral model based on distance from the point of introduction in Brazil, because a single dispersal rate cannot generate predictions that simultaneously fit the clines in North and South America well (see S2 Table).

In addition to these global ancestry estimates, we measure variation in local ancestry frequencies across the genome, which are informative about recent evolutionary history.

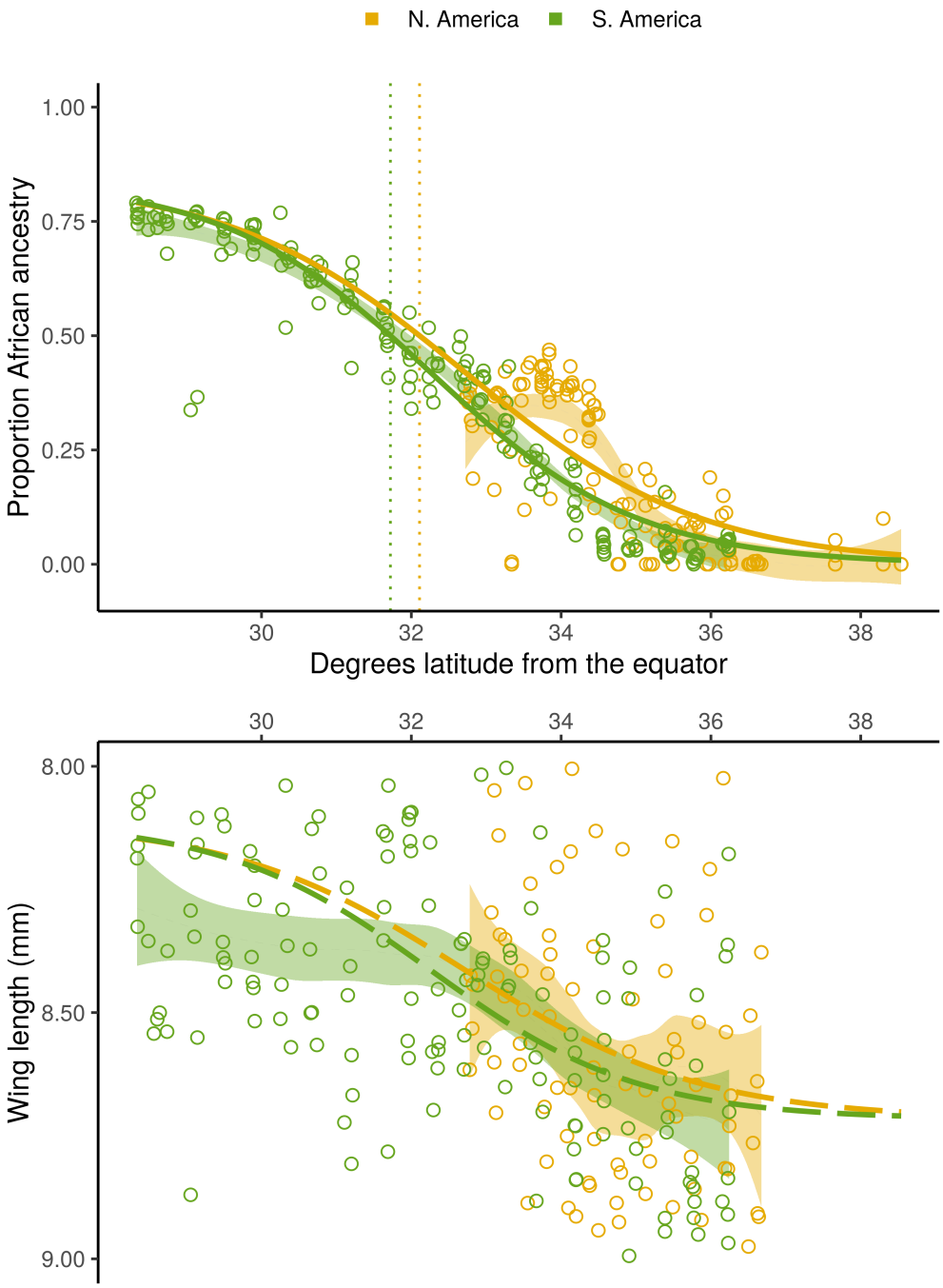

Fig 2. Clines across latitude. Genome-wide ancestry estimates (top) and fore wing lengths (bottom) for individual bees, plotted across absolute latitude and colored by continent. In both panels, shading indicates the 95% confidence intervals for loess curves of the raw data. We also overlay several model-fitted clines: In the top panel, solid curves show the North and South American logistic cline fits for ancestry predicted by latitude, with dotted vertical lines marking the latitude at which bees have predicted 50% African ancestry, based on these curves. In the bottom panel, dashed curves show the expected phenotypic cline if wing lengths were fully determined by the clines in ancestry depicted in the top panel. To get these predicted wing lengths, we used the mean ancestry cline as input to the best-fit linear model between ancestry and wing length. Note that the y-axis for wing lengths is reversed (smaller wings are higher) to simplify visual comparisons between the upper and lower panels.

African ancestry frequencies at individual SNPs vary around their genome-wide mean due to finite sampling, but also evolutionary processes, including drift and selection. If two populations have shared gene flow post-admixture, at SNPs where one population has higher than average African ancestry frequencies, the second population will also tend to have higher than average African ancestry. We capture this genetic signature in an ancestry covariance matrix, where each entry represents how much a pair of populations co-deviate in locus-specific African ancestry away from their individual genome-wide means (Fig 3). We expect ancestry co-variances to build up along each route of the Africanized honey bee invasion as a result of shared drift post-admixture. Indeed, we do observe positive ancestry covariances for nearby populations within each hybrid zone. We attribute this pattern to shared demographic history, but also note that weak selection for a specific ancestry at many loci genome-wide could also generate these positive covariances. Unexpectedly, we find that populations in more temperate North and South America, i.e. at opposite ends of the expansion, have higher ancestry correlations with each other than with populations situated between them. This robust signal is a general pattern that holds true on average across chromosomes (see Fig 14), and so isn't driven by individual outlier loci, and persists across recombination rate bins (see Fig 15). These similar ancestry patterns in geographically distant populations are potentially consistent with a genome-wide signature of convergent selection to cooler climates or convergent selection by beekeepers at higher latitudes.

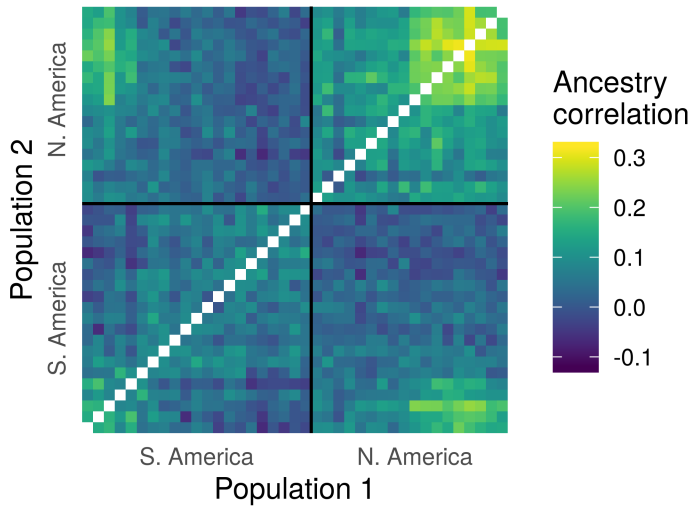

Fig 3. Correlated ancestry across populations. Shared drift in ancestry shown as an ancestry correlation matrix (see methods). Populations are ordered by latitude and diagonals are left blank (within-population correlations = 1).

Genetic basis of the climate barrier

To identify loci that may be contributing to a climate barrier, we looked for SNPs with steeper than expected ancestry clines across latitude in South America. We estimated best-fitting logistic ancestry clines for ∼542k individual loci across the genome by re-fitting eqn. 1 using nonlinear least squares, where x_i is the population latitude and A_i is the population-mean local ancestry at a focal SNP, and the maximum African ancestry M is 1. Because genetic drift will induce variation among loci in their

deviations from the genome-wide cline, we also estimated a distribution of neutral clines from simulations of 100,000 unlinked loci undergoing drift and used these simulated clines to calculate false-discovery-rates. Our simulations are based on a multivariate-normal model, African ancestry $\sim \mathrm{MVN}(\alpha, K)$, where α is the vector of population mean genome-wide A ancestry proportions, and the K matrix measures the expected variance and covariance in ancestry away from this mean (Fig 3), and is empirically calculated using all loci across the genome (see methods for additional details).

We find no evidence to support a simple genetic basis or environmental threshold to the climate barrier. Ancestry clines in South America are reasonably concordant across most SNPs; 95% of cline centers fall within a 1.6 degrees latitude range, with a long tail that appears to be due to adaptively introgressing loci (identified as outliers below, see Fig 10). We find no strongly selected individual barrier loci that exceed our 5% false-discovery-threshold for cline steepness, set by MVN simulation of background ancestry patterns. On average, individual SNP clines in South America are 937km wide (w = 8.44 degrees latitude), and the steepest cline in the genome still takes approximately 555km (w = 5 degrees latitude) to fully transition from African to European ancestry. These wide clines, coupled with the evidence for parallel genome-wide clines in North and South America, are consistent with selection tracking smooth climate transitions over broad geographic regions rather than a discrete environmental step. Furthermore, concordance in clines across SNPs in South America suggests that many loci are associated with climate-based fitness trade-offs. An additional prediction for a polygenic climate barrier is that loci maintaining steeper clines will co-localize in regions of the genome with low recombination, where linked together they form stronger barriers to gene flow than any one locally-adapted locus acting alone [6]. We test this theoretical prediction in South America and find enrichment for steeper clines in regions of the genome with low recombination. The empirical top 5% steepest clines in South America are found on all 16 chromosomes and are enriched in regions of the genome with low recombination. Steep clines comprise 12.7% CI_{95}[8.4%-16.5%] of loci from the lowest recombination rate quintile vs. only 3.3% CI_{95}[3.0%-3.6%] of loci from the highest recombination rate quintile. The average effect of recombination is a 50km decrease in mean cline width between the highest and lowest recombination rate quintiles ($\Delta b = 0.028$, [0.017-0.038]).

Diversity and rapid expansion

From their point of origin in Brazil, Africanized honey bees invaded much of the Americas in less than 50 years [61]. Such rapid expansion can lead to high rates of drift in the continually bottle-necked populations at the front of the wave of expansion, i.e. those populations sampled furthest from Brazil. To test this expectation, we calculated nucleotide diversity, π, for each sampled population (see Fig 4). Despite much further distances traveled to the northern hybrid zone, we do not observe a more pronounced bottleneck in California than in Argentina, suggesting that the expanding wave of Africanized honey bees maintained large population sizes (and did not experience strong 'allele surfing' [22]).

Africanized bee populations are consistently more diverse than reference bee populations because they are genetic mixtures of these diverged groups. We do, however, observe a drop in diversity in the tails of both hybrid zones starting at approximately 34.5° latitude from the equator. We tested whether this drop in diversity is necessarily the result of a bottleneck or can be explained solely by a cline in mean ancestry composition from more diverse African and highly admixed genomes to less diverse European stock. To test this alternative, we predicted population diversity from a simple weighted average of A, C, and M reference allele frequencies and the observed

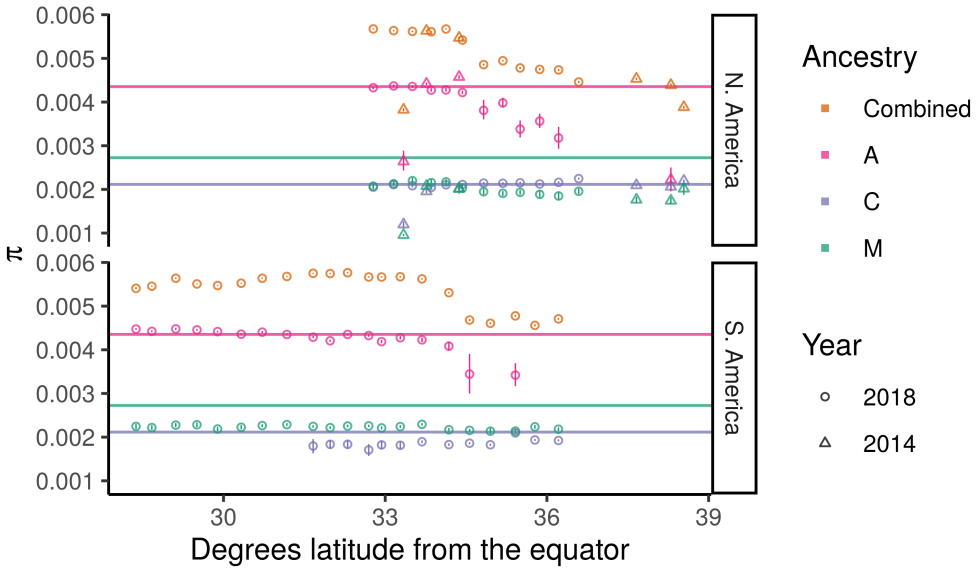

Fig 4. Allelic diversity (π) across the hybrid zones. For each population, we estimated allelic diversity genome-wide and within high-confidence homozygous ancestry states. Horizontal lines show the genome-wide diversity within the reference panels. Vertical lines show the 95% confidence interval for each estimate, based on a simple block bootstrap CI using 1cM blocks. For several populations in the tails of the cline, we do not show A and/or C within-ancestry estimates because these populations have too few high-confidence ancestry blocks for accurate estimation (see methods). The low diversity outlier at 33.34 degrees latitude in the N. American cline is the 2014 Avalon sample, which comes from a small island population off the coast of California.

population ancestry proportions. We find that based on ancestry composition alone, we do expect a drop in diversity across the hybrid zones, although the observed drop is slightly less than our predictions (see Fig 21).

Levels of diversity within European C and M ancestries are similar to the reference panels and stable across latitude, evidence that a diverse population of European ancestry bees hybridized with African bees as they expanded away from Brazil. We also find high diversity within African haplotypes in both hybrid zones, again consistent with no bottleneck associated with the rapid expansion. However, the diversity in the African ancestry background does decline in populations furthest from the equator, which is consistent with either strong filtering of African haplotypes by selection or stochastic haplotype loss due to small African-ancestry population sizes in the tails of the clines.

Scan for ancestry-associated selection.

We identified loci with unusually high African ancestry frequencies, a signal of natural selection, using our MVN simulations of background covariance in ancestry to set a false discovery rate. The ancestry covariances are important to account for when testing for putative selected loci that depart from genome-wide background ancestry patterns, because deviations in ancestry are correlated across populations. Although many population pairs have only small positive ancestry covariances, the cumulative effect on the tails of the distribution of African ancestry frequencies in the larger sample is striking. These covariances can confound outlier tests for selection which only consider variance from sampling (e.g. Poisson-Binomial, e.g. [54]). We find that by incorporating background patterns of shared drift (or weak genome-wide selection) into our null

model, we can match the bulk of the observed ancestry distributions across the genome (see Fig 5).

Loci important to the successful invasion of Africanized honey bees are likely to have an excess or deficit of African ancestry across both continents. Thus, we tested separately for high and low African ancestry outliers on each continent, and then identified overlapping outliers between the two hybrid zones. We find evidence of selection favoring African ancestry at 0.34% of loci in N. America and 0.13% of loci in S. America, across 14 chromosomes (see Fig 6). From these outliers, we find 13 regions with an excess of African ancestry in both hybrid zones at less than a 10% false-discovery-rate (top right corner of Fig 5). The majority (11/13) of shared outliers co-localize within a ∼1.5Mb region on chromosome 1, but within this region outliers separate into multiple distinct peaks (see Fig 6). One way a cluster of African ancestry peaks could form is if favored African alleles experience additional indirect selection from being in linkage disequilibrium with other favored African alleles at nearby loci, thereby increasing the total effective selection in a region [6]. While ancestry-informative markers (AIMs) with fixed or nearly fixed differences between African and both European ancestries are relatively rare, we were able to confirm the highest A peak within this cluster using AIMs outside of the local ancestry inference SNP set (see Fig 16). African alleles at this main peak appear to have introgressed to high frequency hundreds of kilometers past the hybrid zone centers in both North and South America, but not reached fixation in any population (see Fig 7). The rapid rise and slow fixation of this allele is potentially consistent with dominant fitness benefits. How far these African alleles have introgressed past the present hybrid zones is currently unknown because they exceed our range of sampling.

Our goal was to identify regions of the genome where high fitness is broadly associated with African ancestry, but an alternative explanation for high African ancestry at a locus is that a very recent adaptive mutation just happened to fall on an African haplotype, initiating a classic 'hard sweep'. For shared high African-ancestry outlier regions, we distinguished between these two scenarios using population differentiation (F_{ST}) within A ancestry. We analyzed differentiation across the large cluster of shared high African-ancestry outlier peaks on chromosomes 1 and across a smaller region on chromosome 11 that contains the other two high African ancestry outliers shared between continents. We did not find high allelic differentiation between North and South American A ancestry tracks and the A reference panel (see Figs 18 and 19), suggesting that African ancestry in general, and not one particular haplotype, was favored by natural selection at these loci.

We used previous literature and gene orthologs to identify possible adaptive functions for regions of the genome where selection has favored African ancestry. There are 3 major quantitative trait loci (QTLs) associated with defense behaviors (e.g. stinging) in genetic crosses of Africanized and European bees [37,38], none of which overlap any signatures of selection from this study. No studies have mapped the genetic basis of elevated *Varroa* defense in Africanized (vs. European) bees, but we were able to compare our results to quantitative trait loci (QTLs) associated with anti-*Varroa* hygiene behaviors [55,67,76] and defensive grooming [4] more generally. The cluster of peaks for high shared African ancestry on chromosome 1 overlaps a putative QTL associated with removal of Varroa-infested brood [67], but there are a number of large QTLs in the genome. A total of 104 genes overlap high African ancestry outlier peaks. Predicted functions for these genes (primarily based on fly orthologs) are not significantly enriched for any Gene Ontology (GO) categories, which may simply reflect that many outlier regions are broad and contain many genes, most of which are likely unrelated to their rise in ancestry frequency. A smaller set of 37 genes with high African ancestry have signatures of selection on both continents. For these, we searched the

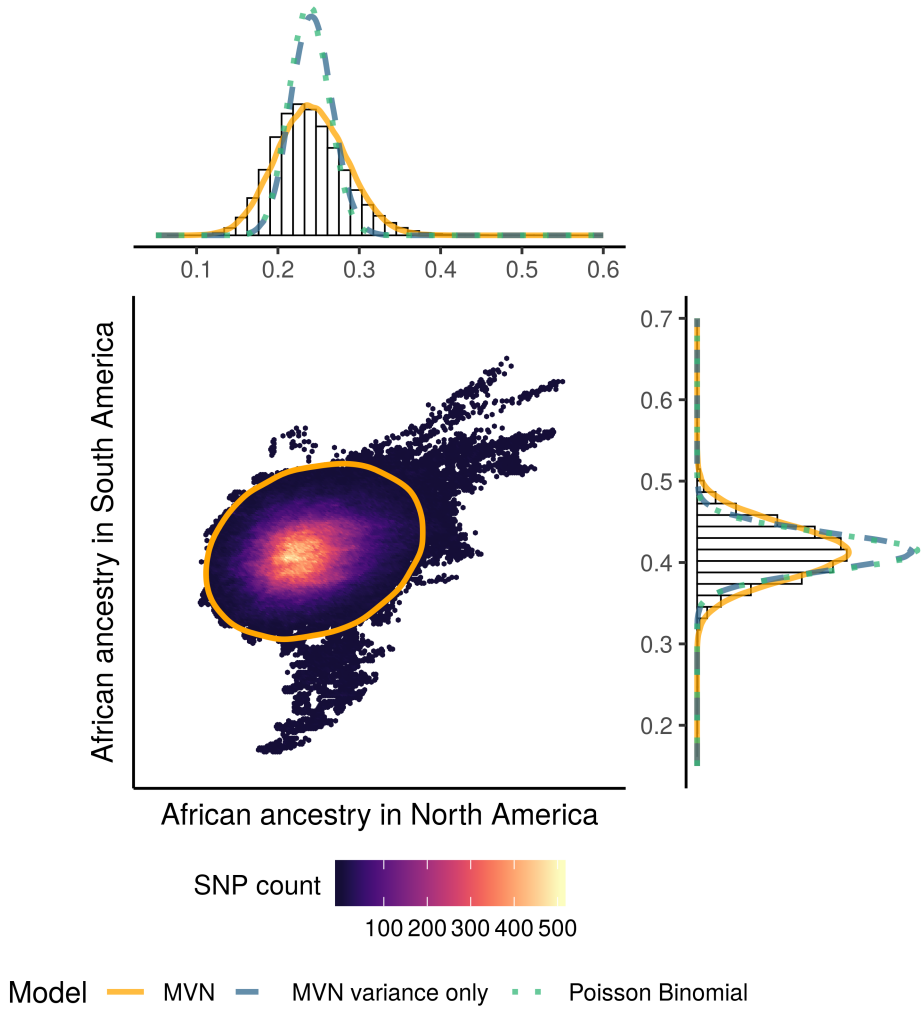

Fig 5. Local ancestry outliers compared across hybrid zones. We plot mean African ancestry frequency in North vs. South America for 425k SNPs across the honey bee genome. SNPs are binned for visualization, and colored by the number of SNPs within each hex. Outside the axes, we show the marginal histograms of African ancestry for each continent separately. On top of these histograms, we plot density curves for 3 possible null distributions for ancestry frequencies: the full MVN model which accounts for drift in ancestry both within and between populations, a variance-only MVN model which only accounts for drift within populations, and a Poisson-Binomial model which only includes sampling variance. Most neutral SNPs are expected to fall within the orange circle, which delineates the approximate 99% highest posterior density interval based on full MVN simulations of background ancestry patterns. SNPs in the top right, with higher than expected African ancestry proportions in both hybrid zones, are our best candidates for loci underlying adaptive African-ancestry associated traits.

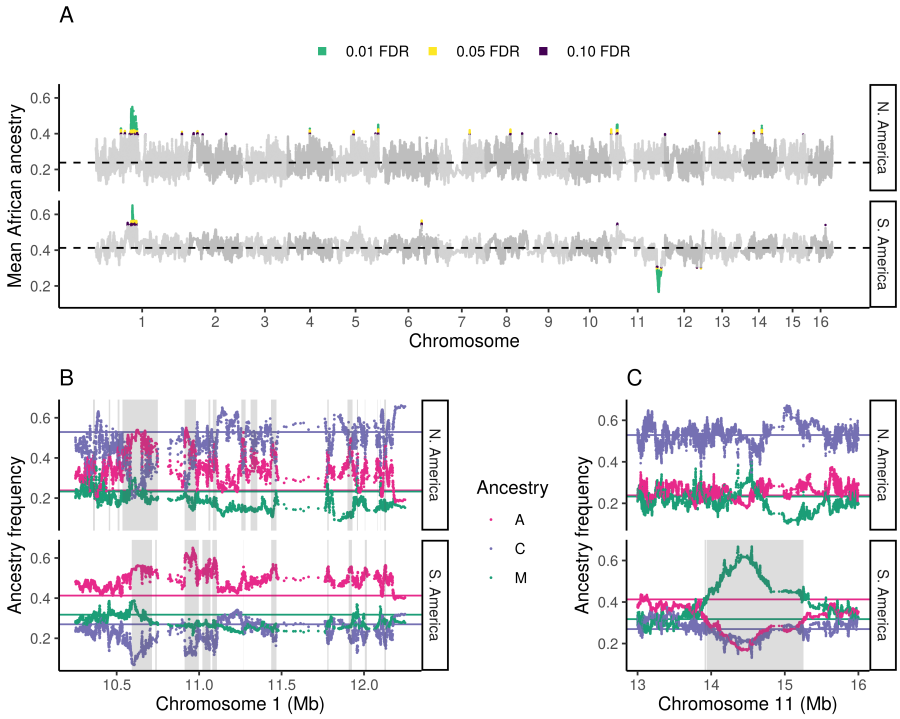

Fig 6. Genomic location of ancestry outliers. A. Mean African (A) ancestry in each hybrid zone at SNPs across the genome, with outliers colored by their false-discovery-rate. Genome-wide mean African ancestry in each zone is indicated with a dashed line. Shared peaks for high African ancestry are seen on chromosomes 1 and 11; there are no shared peaks for low A ancestry. B. Zoomed in view of cluster of shared high African ancestry outliers on chromosome 1, with European ancestry separated into eastern (C) and western (M) subtypes. Genome-wide mean frequencies for each ancestry are shown with colored lines. Outlier regions meeting a 10% FDR for high A ancestry are shaded in grey, with additional 1kb buffering for visibility. Shared outliers between continents overlap between the top and bottom panels. C. Zoomed in view of the high M European ancestry outlier region found in South America. Outlier regions for low African ancestry (<10% FDR) are shaded in grey. Note: The x-axis scale differs between plots.

literature and found that two have been associated with *Varroa* in previous studies: a myoneurin (LOC725494) that is overexpressed in the brains of *Varroa* infected worker bees compared to *Nosema* infected bees and controls [49] and an uncharacterized protein (LOC725683) that is over-expressed in parasitized drones compared to non-parasitized drones [68]. While these are potentially intriguing candidates for selection, *Varroa* is only one of many possible selective pressures, and more work is needed to link the signals of selection we find here to adaptive functions.

In contrast to high African ancestry outliers, we do not find any shared outliers for European ancestry. However, the most striking example of a single-zone selection event is a large 1.4Mb region on chromosome 11 with excess European ancestry in South America (bottom middle of Fig 5). This region was previously identified to have low African ancestry in Africanized honey bee populations from Brazil [54]. We independently identify this region as a low African-ancestry outlier across Argentina, using different A/C/M reference bees, ancestry calling algorithm, and bee samples than

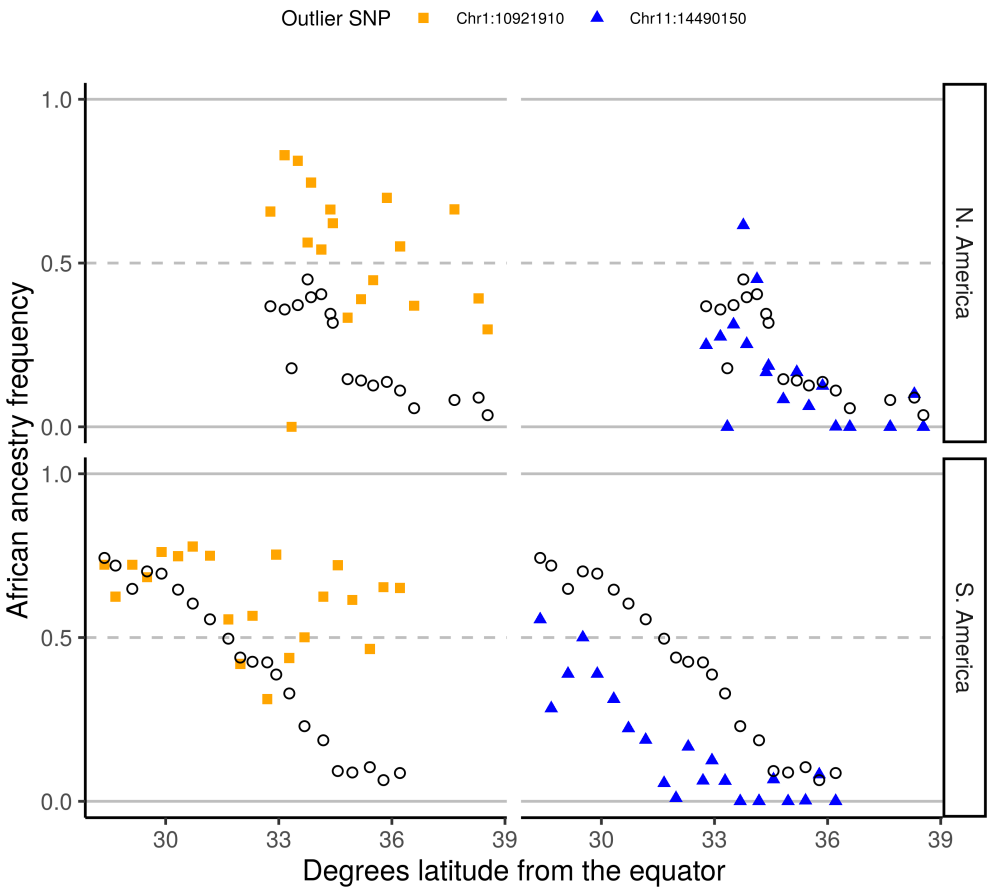

Fig 7. Ancestry clines at outlier SNPs. At two top outlier SNPs, we show the clines for mean population African ancestry across latitude in North (top) and South (bottom) America. Genome-wide mean local ancestry calls for each population are shown for comparison as black circles. To the left, we show the ancestry cline for the SNP with the highest African ancestry in the combined sample, located within the top peak on chromosome 1 for high shared African ancestry across continents. To the right, we show the ancestry cline for the SNP with the lowest African ancestry in South America, located within the large outlier region on chromosome 11 for high M and low A ancestry.

the previous paper. We find that populations across the South American hybrid zone have reduced African ancestry at this locus, but that North American populations do not appear to have experienced selection (see Fig 7). By including C-lineage diversity in our admixture analysis, we additionally show that this region is specifically elevated for M haplotypes, and not European haplotypes more broadly (see Fig 6). This region has many diverged SNPs between the three ancestry groups beyond the SNPs included in our ancestry_hmm analysis, which we use to confirm high rates of M introgression (see Fig 17). It does not appear that a new mutation or narrow set of haplotypes was favored within M because we see little differentiation between the M ancestry in this selected region compared to the M reference panel. Additionally, within the selected region we find a peak of high F_{ST} between A, C, and M reference panels (see Fig 20), which is consistent with this region having historically been under selection within these ancestry groups. Finally, the California bees do not have a significant deficit of African ancestry like the Argentinian bees do, but they do have two narrow peaks of excess M ancestry within this region, in the top 3% and 7% empirical percentiles for M ancestry genome-wide. Our data support a scenario in which a diversity of M haplotypes carrying the favored allele were driven to high frequency in South America after Africanized honey bees spread north of Brazil. Potential candidate genes specific to this large M-ancestry outlier region on chromosome 11 are previously described by [54]. In total, we find 186 genes that overlap low African ancestry outlier peaks (<10% FDR). These genes are not functionally enriched for any Gene Ontology (GO) categories.

Discussion

The introduction of African honey bees to Brazil in the 1950s sparked one of the largest and best studied biological invasions known to date, spreading from a single point of release over much of the Americas in less than 50 years. We add to this literature the first comparative study of the invasions in North and South America, with genome-wide resolution on the present distribution of African ancestry.

The parallel alignment of the genome-wide cline with latitude in both continents, despite very different length dispersal routes, strongly supports the view that African-ancestry has reached a stable climatic range limit. Because our transect in California only covered the upper half of the North American cline, the full shape for this genome-wide cline is uncertain, and may be asymmetrical because one signature of a moving hybrid zone is elongation of the lagging tail [10]. In contrast, we have strong evidence for convergence in the low-African portions of these two genome-wide clines, which are not expected to be distorted by cline movement, and reflects similar latitudinal range limits for African ancestry in North and South America. Global warming trends could shift the location of the observed clines towards the poles, as has been documented for other hybrid zones sensitive to climate change [72]. While we currently lack temporal data with comparable genomic and geographic resolution, our results can be used as a baseline for future study.

We observe relative uniformity at the climate barrier, with no individual loci showing steeper ancestry clines than what can be produced by a null model accounting for background patterns of variation in ancestry frequencies shared across populations. Nor do we observe any loci that have below 10% frequency of African ancestry in California, despite the large distance and climatic range traveled over by this portion of the invasion. If the invasive ability of Africanized bees were due to a small number of loci we would expect African ancestry to have been swamped out at many unlinked neutral loci in the genome due to interbreeding at the front of the advancing wave of expansion [15]. Instead, relative genomic cohesion points to a broad genetic basis for the high fitness and rapid spread of African ancestry as well as the fitness costs in cooler

climates underlying the parallel range limits observed across continents. However, we note that the distinction between Africanized and non-Africanized honey bees is likely to further blur over time. Genetic barriers are strengthened when selection is distributed across many loci, but they are still easily permeated by adaptive alleles [5]. Furthermore, given high recombination rates in honey bees, we predict only loci tightly associated with climate-based fitness trade-offs will remain geographically bounded over long periods of time.

Significant effort has been focused on finding an environmental isocline that divides regions where Africanized honey bees are expected to dominate and regions where they cannot overwinter (e.g. [31, 62, 66, 73]). However, we observe ancestry clines that are hundreds of kilometers wide, not the narrow clines created by strong selection across a discrete environmental transition. Theoretically, these broad clines could be consistent with neutral diffusion of ancestry by migration over tens of generations. However, a scenario of neutral diffusion is inconsistent with external evidence of the rapid spread of the invasion and strong fitness trade-offs with climate: the high competitive advantage and very rapid advance of Africanized honey bees in the tropics in the face of considerable interbreeding with European bees and, conversely, documented low fitness in cooler climates, with low overwinter survival and maladaptive metabolic efficiency, foraging preferences and nesting behaviors (see [31] for a review). Thus, we conclude that honey bee fitness is more likely to be tracking environmental variables with smooth transitions over broad geographic regions (e.g. climate), which may create intermediate environments where ancestry intermediates have higher fitness, thus broadening the observed hybrid zones, similar to the dynamics in other hybrid zones spanning broad ecotones [21, 25].

We sampled an abundance of bees with intermediate African ancestry proportions, which implies that Africanized honey bees cannot be treated as a single genetically and phenotypically cohesive group. Rather, as a null model, we expect phenotypic clines to match the scale of the observed ancestry clines, with smooth transitions in mean phenotype over hundreds of kilometers. Many phenotypes of interest, e.g. defensive behavior or *Varroa* tolerance, are expressed or measured at the colony-level and so we could not assess these in our survey of freely foraging bees. Future phenotypic surveys could be compared with our genomic clines to ascertain if key phenotypes diverge from this expected pattern, e.g. due to strong selection beyond that experienced by the rest of the genome. Indeed we see that wing length, a trait hypothesized to be associated with latitudinal body-size adaptation following Bergmann's rule [18], has a geographic distribution consistent with the genome-wide ancestry cline. This suggests that while wing length, which is strongly correlated with body size [17, 58], may well have fitness trade-offs with climate, selection for these traits does not appear to be strong enough compared to average selection for ancestry to deviate from background genomic patterns over a short time scale.

Using wing length as an example, we show how the genomic patchwork of ancestry and ancestry-associated traits in Africanized honey bees can be leveraged to study the genetic basis of phenotypic adaptation in these wild populations. While our admixture mapping study did not identify any large effect loci for wing length, this approach can be readily applied to other measurable traits of interest with genetic differences between European and African honey bees, including defensive behaviors [37–39], foraging preferences [23, 37], body size [38], overwintering-success [79, 85] and *Varroa* tolerance [50, 53, 78]. Admixture mapping studies in Africanized honey bee populations are expected to deliver high genomic resolution on the order of 100kb, as a result of high recombination rates (24cM/Mb [40]) and over 60 years of admixture.

Africanized honey bees provide a promising source of genetic variation for breeding in light of the vulnerability of European lineages to current environmental stressors and

the associated bee declines [26]. Africanized honey bees have high competitive fitness and, we show here, maintained high genetic diversity despite their rapid expansion. However, a targeted approach is needed to identify high fitness African alleles that are promising for breeding within a background that segregates for undesirable traits such as defensive behaviors. In this study, we have taken a first step towards mapping the genetic basis of the high fitness of Africanized honey bees by identifying loci where selection has favored African or European ancestry in both North and South America. We identify several loci with convergently high African ancestry on both continents, and many more across the genome with evidence of selection favoring African ancestry in one hybrid zone. In contrast, with the exception of one striking outlier for high M ancestry in South America, we find little evidence that European ancestry or admixture per se contributed broadly to the success of Africanized honey bees. We attribute this difference in results from a previous study of Africanized honey bees in Brazil [54] to a more appropriate null model that accounts for shared variance in ancestry across populations. While our population genetics approach is trait-blind, our results can be compared to future functional and genetic mapping studies to look for overlap between trait-associated and positively selected loci. Applying similar methods to other non-model systems, especially where replicated hybrid zones can be sampled, holds great promise for revealing loci important to adaptation.

Materials and methods

Sampling

We sampled individual foraging honey bees across two hybrid zones, located at the transitions to temperate climates in North and South America. We sampled at least 10 bees each from 12 populations in California and 21 populations in Argentina (see maps, Fig 1).

For each population, we hand-netted individual foraging bees within a sampling radius of approximately 15km. Because commercial colonies are often temporarily relocated for the spring pollination season, we sampled in summer, when foraging bees are more likely to come from resident populations. We additionally included in our analyses 35 high-coverage published genomes of freely foraging bees collected from 6 populations between September 2014 and January 2015: Davis, Stebbins, Stanislaus, Avalon (Catalina Island), Placerita, and Riverside (Sky Valley and Idyllwild) [13]. While these sampled bees come from an unknown mixture of local feral and domesticated colonies, previous surveys from California have found that freely foraging bees tend to closely match feral sources, based on mtDNA composition [43]. Consistent with this view, eight of our sequenced bees from different populations in Argentina were collected close to a feral nest (< 5m), but do not appear to be ancestry outliers for their sampling locations. More specifically, we fit a general linear model (logit(African ancestry) $\sim$ absolute latitude + feral nest) using glm with gaussian errors in R and found no significant effect on African ancestry of sampling near a feral nest ($P = 0.97$). Based on these results and our seasonal timing, the bees in this study are likely sourced primarily from local feral populations, with some contribution from resident domesticated bee colonies.

Lab work and sequencing

We selected a subset of 279 bees from our North and South American hybrid zones for whole genome sequencing, 8-9 bees per sampled population (see S1 Table). For each bee, we dissected wing flight muscles from the thorax and extracted DNA using QIAGEN

DNeasy Blood and Tissue kits. We followed a new high-throughput low-volume DNA library preparation protocol (see [59] for details "Nextera Low Input, Transposase Enabled protocol"). Briefly, we prepared individual Nextera whole-genome shotgun-sequencing DNA libraries using enzymatic sheering and tagmentation. Then we PCR-amplified and barcoded individual libraries using the Kapa2G Robust PCR kit and unique custom 9bp 3' indices. Finally, we pooled libraries within each lane and ran bead-based size-selection for 300-500bp target insert sizes. We targeted 4-6x coverage per bee based on a preliminary analysis of our power to replicate local ancestry calls from one of the published high coverage populations (Riverside 2014) using simulated low coverage data (see Fig 4). We multiplexed our samples across 5 Illumina HiSeq4000 lanes for paired-end 2 x 150bp sequencing. In total, we generated 5.1x mean coverage per bee for 278 samples. The 279th sample was excluded from all analyses for having extremely low (<0.1x) sequence coverage.

Alignment and SNP set

In addition to the sequence data produced by this study, we downloaded Illumina raw read sequences for 35 previously published California genomes (PRJNA385500 [13]) and a high-quality reference panel of African (n = 17), eastern European (n = 9) and western European (n = 9) honey bee genomes (PRJNA216922 [30] and PRJNA294105 [14]) from the NCBI Short Read Archive. For all bees, we mapped raw reads to the honey bee reference genome HAv3.1 [80] using Bowtie2 very-sensitive-alignment with default parameters [45]. We then marked and removed duplicate reads with PICARD and capped base quality scores using the 'extended BAQ' option in SAMtools. Using the software ANGSD [44], we identified a set of SNPs with minor allele frequency $\geq 5\%$ in the combined sample based on read counts (-doMajorMinor 2 -doCounts 1). For SNP calling, we applied standard quality filters (base quality ≥ 20, mapping quality ≥ 30, total read depth ≤ 5500 ($\sim$2x mean), and coverage across individuals $\geq 50\%$).

Global ancestry inference

We estimated genome-wide ancestry proportions for each bee using methods designed for low-coverage sequence data. Briefly, we combined bee genomes from the hybrid zones with reference genomes from Africa (A), eastern Europe (C) and western Europe (M). To reduce LD (non-independence) between our markers for global ancestry inference, we thinned to every 250th SNP ($\sim$14k SNPs at 19kb mean spacing) before calculating genotype-likelihoods for each bee using the SAMtools method in ANGSD (-GL 1). We first ran a principal components analysis in PCAngsd [51] to confirm that genetic diversity in the hybrid zones is well-described by 3-way admixture between A, C, and M reference panels (see Fig 1). We then estimated genome-wide ancestry proportions for all bees using NGSAdmix (K = 3) [65].

Local ancestry inference

We inferred the mosaic of African vs. European ancestry across the genome of each bee using a hidden Markov inference method that can account for African (A), eastern European (C) and western European (M) sources of ancestry within low-coverage Africanized honey bee genomes (ancestry_hmm [12]). For local ancestry inference, we enriched for ancestry-informative sites by filtering for ≥ 0.3 frequency in one or more reference population (A, C, or M) and at least 6 individuals with data from each reference population. We subsequently thinned markers to 0.005cM spacing, because at that distance LD within ancestries is expected to be low ($r^2 < 0.2$ [81]), leaving a final

set of 542,655 sites for ancestry calling, or $\sim 1/7$ of the original SNP set. Individual bees sequenced in this study, and previously published California bees, have 5.42x and 14.5x mean coverage, respectively, across this final SNP set. For each population, we jointly estimated time since admixture and ancestry across the genome of each individual, using read counts from the hybrid zone, a 10kb-scale recombination map [40], and allele frequencies for European and African reference populations at each SNP. To generate major/minor allele counts for each reference population, we used ANGSD to call genotypes (-doPost 1) using a minor allele frequency prior (-doMaf 1) and the SAMtools genotype likelihood (-GL 1), after quality filtering (map quality ≥ 30, reads matching major/minor allele $\geq 60\%$, and read depth $\geq$ 6x). As additional inputs to ancestry_hmm, we used NGSAdmix results as a prior for population ancestry proportions and set the effective population size to $N_e = 670,000$ [54]. We modelled a simple three-way admixture scenario: starting with C ancestry, we allowed for a migration pulse from M and a second, more recent, migration pulse from A. Timing of both migration pulses were inferred from the range 2-150 generations, with priors set at 100 and 60 generations. To calculate a point estimate for each individual's ancestry proportion at a SNP, we marginalized over the posterior probabilities for homozygous and heterozygous ancestry from the ancestry_hmm output (i.e. $A = p(AA) + 1/2(p(CA) + p(MA))$.

African ancestry covariance matrix

To explore how populations vary and covary in their African ancestry along the genome we calculated the empirical population ancestry variance-covariance matrix (K), an admixture analog of a genotype coancestry matrix (e.g. [75]). The K matrix is calculated using population African ancestry frequencies inferred by the local ancestry HMM, e.g. for populations i and j with mean ancestry proportions α_i and α_j, and ancestry frequencies at a locus $anc_{i,l}$ and $anc_{j,l}$, their ancestry covariance calculated across all L loci genome-wide is

$$K[i,j] = \frac{1}{L}\sum_{l=1}^{L}(anc_{i,l} - \alpha_i)(anc_{j,l} - \alpha_j).$$

Simulated ancestry frequencies

At various points in the results we compare our outliers to those generated by genome-wide null models of ancestry variation along the genome. We simulated variation in ancestry frequencies at SNPs across the genome under three models: (1) A poisson-binomial model that only accounts for sampling variance, not drift (e.g. [54]); (2) a multivariate-normal model with covariances set to zero, which accounts for effects of both sampling and drift within-populations (e.g. [47]); and (3) a multivariate-normal model with covariances to additionally account for shared drift in ancestry between populations. For each model, we simulated in R neutral African ancestry frequencies at 100,000 independent loci. The full multivariate-normal model is used for comparison to the results, while the first two models are only used to show the effects of ignoring covariances.

In the Poisson-Binomial simulation, for each bee we sampled 2 alleles from a binomial distribution with mean equal to the individual's genome-wide ancestry proportion inferred by ancestry_hmm.

For the variance-only MVN simulation, we empirically calibrated an independent normal distribution for each population that can exceed binomial ancestry variance (e.g. due to drift). This model is equivalent to the full MVN model below, but sets all off-diagonal entries of the K ancestry variance-covariance matrix to zero.

In our full multivariate-normal model, we account for non-independent ancestry within and between our sampled populations:

$$\text{African ancestry} \sim \text{MVN}(\alpha, K),$$

where α is the vector of genome-wide mean population ancestry frequencies and K is the empirical population ancestry variance-covariance matrix. Because the MVN models are not bounded by 0 and 1, but real frequency data is, we set all simulated individual population frequencies exceeding those bounds (5.2% low and 0.09% high) to the bound. Truncation has little effect on the distribution in general and no effect on the frequency of high African ancestry outliers, but does make extremely low outliers (attributed to some populations having simulated negative frequencies) less likely (see Fig 11). For more details on model approximations to the observed data, see Figs 12 and 13.

Cline models

To better understand the role of dispersal and selection maintaining the current geographic range limits of Africanized honey bees, we fit a logistic cline model to the individual genome-wide ancestry proportions estimated by NGSAdmix. We estimated continent-specific c and b parameters to test for a difference in cline center (degrees latitude from the equator) and/or slope between the northern and southern invasions. Then we fit a joint model with a single cline to see how well absolute latitude or climate can consistently predict African ancestry frequencies across both continents. Specifically, we tested three environmental variables that likely contribute to varying fitness across space: mean annual temperature (°C), mean temperature of the coldest quarter (°C), and mean annual precipitation (cm). We downloaded mean climate observations for 1960-1990 [32] from WorldClim.org at 30 second map resolution (≈ 1 km^2 at the equator) and then averaged within a 5km radius around each bee's sample coordinates. We compared climate and latitude-based selection models to a neutral dispersal model, where genome-wide African ancestry is predicted solely based on the distance (km) traveled from Río Claro, São Paulo, Brazil, the point of origin for the Africanized honey bee invasion (estimated from GPS coordinates, "distGeo" in R). For each model, we substituted latitude, distance, or climate for x_i in Eq 1 and we used AIC to compare model fits.

We then fit individual-SNP clines to the mean population ancestry frequencies in South America, where our samples span the full cline. We tested for individual outlier loci that may underlie a climate barrier by fitting the same logistic cline model to a set of simulated population ancestry frequencies for S. America (see MVN simulation), and comparing observed cline slopes to this null distribution. In addition, we tested for enrichment of the empirical top 5% of steep clines in regions of the genome with low recombination rates. We divided the genome into 5 equal-sized recombination rate bins ([0, 2.92], (2.92, 21.6], (21.6, 31.7], (31.7, 38.6] and (38.6, 66.9] cM/Mb) and used 10,000 block bootstraps [8] to calculate basic bootstrap confidence intervals for each quintile while accounting for spatial correlation in both cline slopes and recombination rates across the genome. For the bootstrap, we divided the genome into 0.2cM blocks, we re-sampled these blocks with replacement, and for each recombination bin we calculated mean b and the proportion of SNPs in the top 5% steepest slopes from our bootstrap sample. When fitting non-linear least squares in R for both genomewide and individual snp clines, we used multiple random starting values to make sure we searched across all local minima and found the global optimum solution (nls.multstart). Starting values were drawn from uniform distributions: b $\sim$ Unif(-5, 5) and $\sim$ Unif(min, max) across the observed range for latitude and climate variables.

Wing morphology

We imaged a slide-mounted fore wing and measured wing length to the end of the marginal cell using imageJ (see Fig 8). We included 269 bees in the wing analysis (only bees sequenced by this study had wings preserved and n = 9 bees were excluded for wing tatter or damage).

We also measured fore wing lengths for A, C, and M reference bees in the Oberursel Collection sampled from their native range (n = 52 [60]). While the effect of ancestry on wing length is similar in magnitude and direction in both datasets, we found that the mean wing lengths for the European reference bees (C & M) fell below the mean for our American bees with close to 100% European ancestry, perhaps reflecting phenotypic plasticity. Thus we do not incorporate these measurements of A, C, and M reference bees into the subsequent analyses.

We tested various models of the relationship between wing length, ancestry and geography. First, we fit a linear model to predict wing length in our sample from genome-wide ancestry. We visually compared our wing measurements to what we would expect if the cline in wing length across latitude were fully described by this linear relationship between ancestry and wing length and our best-fit clines for genome-wide ancestry (see Fig 2). We additionally tested for differences between continents by adding a main effect and an interaction term for South America to our linear model.

We performed admixture mapping of wing length to test if the ancestry state at any individual SNP predicts residual variation in wing length. To do this, we first regressed wing length on genome-wide African ancestry, to correct for background ancestry effects. We then took the residual wing lengths from this linear model fit and regressed these on African ancestry allele counts at each locus in turn (using the maximum a posterior probability (MAP) estimates from the local ancestry HMM). We set a genome-wide significance threshold of $p < 1.1 \times 10^{-6}$ to control for multiple testing at a 5% family-wise error rate, using an analytical approximation for admixture mapping, calculated assuming 47.6 generations since admixture [27, 63].

Identifying ancestry outlier regions and genes

To identify loci underlying ancestry-associated fitness differences, we tested SNPs for an excess or deficit African ancestry within each hybrid zone. We calculated 1%, 5% and 10% false-discovery rates (FDR) by using our MVN simulation results to set the number of false-positives we expect under a neutral model for high and low African ancestry within each continent separately (one-tailed outlier tests). We then compared the overlap in outliers between hybrid zones to identify SNPs with signatures of selection on both continents.

In addition to local ancestry, we used ancestry-informative markers with fixed or nearly fixed differences to verify high-introgression regions. We defined ancestry informative markers as SNPs with coverage for at least 5 individuals from each reference panel and > 0.95 allele frequency differences between the focal ancestry and both other ancestries. We estimated allele frequencies at each ancestry-informative marker using ANGSD, polarized SNPs so the focal ancestry has the highest MAF, and only included markers with coverage in all sampled populations. Ancestry-informative markers for A (n = 4,302) are relatively rare compared to markers for C (n = 17,384) and M (n = 15,626) because European populations each experienced a historical bottleneck differentiating them from the other two groups. Because of LD-thinning before local ancestry inference, 88% of these ancestry-informative markers were not included in the ancestry_hmm SNP set, and therefore provide separate support for high-introgression regions.

We identified a set of candidate genes that overlap regions of the genome with

exceptionally high or low African ancestry (<10% FDR) using BEDtools. For this analysis, we downloaded gene annotations for the HAv3.1 genome assembly from NCBI (accessed 7/22/19). 72 out of 104 genes overlapping high African ancestry peaks and 131 out of 186 genes overlapping low African ancestry peaks have associated BEEBASE gene IDs. For these high and low gene sets, we tested for enrichment of Gene Ontology (GO) terms compared to a background of all honey bee genes, using DAVID 6.8 [35] and a Benjamini-Hochberg corrected FDR of 5%. To find out what is previously known about the 37 genes that overlap regions with high African ancestry on both continents, we conducted a literature search using the NCBI gene search tool and google. We additionally checked if our candidate selected loci fell within regions of the genome previously associated with defensive or anti-*Varroa* behavioral traits (QTLs from [4, 37, 55, 67, 76]). We estimated genome coordinates for these QTLs using the best blast hits [3] to HAv3.1 for QTL markers (see S5 Table). When assessing physical overlap between genome annotations and ancestry outliers, we assumed ancestry calls for a SNP apply to the short genomic window around that SNP, spanning midway to the next ancestry call. When visualizing and counting the number of selected regions in the genome, we further merged near-adjacent (<10kb) significant ancestry windows into contiguous regions.

Population diversity

We calculated allelic diversity (π) for each population and our A, C, and M reference panels. First, we calculated a simple unbiased population allele frequency in ANGSD based on a weighted average of observed read counts (counts -8) for each SNP. For this analysis, we included all SNPs ascertained in the combined sample (see 'Alignment and SNP set' above) but excluded SNPs from a population's estimate when fewer than two individuals had coverage. Using these allele frequency estimates, and a finite-sample size correction ($n = 2\times$ number of individuals with data at a site), we calculated mean per-SNP heterozygosity. To approximate uncertainty in our estimates, we divided the genome into 5,254 non-overlapping 1cM blocks, re-calculated our diversity estimates for 10,000 block bootstrap samples, and calculated a 95% simple bootstrap confidence interval. Finally, to get per-bp diversity, we scaled our per-SNP diversity estimates by the density of SNPs in the genome, using the same coverage and depth quality filters in ANGSD as in our SNP pipeline to count total mappable sites.

For within-ancestry diversity estimates, we used our ancestry calls to identify contiguous tracts with high posterior probabilities (>0.8) of homozygous A, C, or M ancestry. We used these tracts to divide the genome into high confidence A, C, and M ancestry states, and filter for reads that mapped within these states. We then repeated the estimation and block bootstrap procedure above using only the reads associated with a particular ancestry. To estimate within-ancestry diversity for a population, we required data for at least 75 1cM blocks spread across at least 15 of the 16 chromosomes, which excludes 6 populations with too little A ancestry in the tails of both clines and 8 populations with too little C ancestry in the S. American cline for accurate estimation. We compared observed and predicted heterozygosity for each population based on expected allele frequencies calculated by multiplying population-specific admixture proportions by reference population allele frequencies for each ancestry.

To test whether selection had favored specific haplotypes, or African ancestry more generally, within shared outlier regions for high African ancestry, we calculated population differentiation (F_{ST}) between the A reference panel and A haplotypes within each hybrid zone. We also calculated within-ancestry F_{ST} between the two hybrid zones, to assess whether the same A haplotypes rose in frequency on both continents. Likewise, for the large high M outlier on chromosome 11, we calculated pairwise differentiation within M ancestry between North America, South America, and the M reference panel.

We similarly calculated F_{ST} for all three contrasts between A, C, and M, reference panels across these outlier regions, to test for signatures of historical selection and divergence between these ancestry groups. For F_{ST} calculations, we estimated within-ancestry allele frequencies for North and South America using the same method described above for within-ancestry π, except pooling individuals by hybrid zone rather than population. We used Hudson's estimator for F_{ST} (Eq 10 in [7]), calculated the average per-SNP F_{ST} within sliding 50kb windows stepping every 1kb across ancestry outlier regions, and only included SNPs with coverage for at least two individuals for both populations in the contrast and windows with at least 10 SNPs.

Acknowledgements

The use of bee samples from Argentina was made possible through collaboration with the National Institute of Agricultural Technology (INTA), Balcarce, Argentina. We thank California Fish and Wildlife for permission to collect honey bees in California. Thank you to Stefan Fuchs and the Oberursel Collection for sharing wing images of A, C and M reference bees. Thank you to Julie Cridland and Nicholas Saleh for early tips on sampling and California bees, to Philipp Brand, Brenda Cameron, and Anne Lorant for sharing protocols and advice on lab work, to Jodie Jacobs and Petra Silverman for help phenotyping wing traits, and to Kelsey Lyberger, Roisin McMullen and Jodie Jacobs for their help in the field netting bees. Thank you also to Brock Harpur and Daniela Zarate for insightful discussions about Africanized honey bees and to members of the Coop and Ramírez labs for helpful input on the project.

Funding

This work was funded by the National Institute of General Medical Sciences of the National Institutes of Health (NIH R01 GM108779, awarded to GC), the Division of Integrative Organismal Systems from the National Science Foundation (NSF No. 1546719, awarded to GC), the North American Pollinator Protection Campaign and Pollinator Partnership (NAPPC Honey Bee Health Grant, awarded to EC and SR), and the Center for Population Biology UC Davis (Pengelley Award, awarded to EC).

References

1. A. H. Abrahamovich, O. Atela, P. De la Rúa, and J. Galián. Assessment of the mitochondrial origin of honey bees from Argentina. *Journal of Apicultural Research*, 46(3):191–194, Mar. 2015.

2. M. N. Agra, C. A. Conte, P. M. Corva, J. L. Cladera, S. B. Lanzavecchia, and M. A. Palacio. Molecular characterization of Apis mellifera colonies from Argentina: genotypic admixture associated with ecoclimatic regions and apicultural activities. *Entomologia Experimentalis et Applicata*, 166(9):724–738, Sept. 2018.

3. S. F. Altschul, W. Gish, W. Miller, E. W. Myers, and D. J. Lipman. Basic local alignment search tool. *Journal of molecular biology*, 215(3):403–410, Oct. 1990.

4. M. E. Arechavaleta-Velasco, K. Alcala-Escamilla, C. Robles-Rios, J. M. Tsuruda, and G. J. Hunt. Fine-scale linkage mapping reveals a small set of candidate genes influencing honey bee grooming behavior in response to *Varroa* mites. *PLoS ONE*, 7(11):e47269, 2012.

5. N. Barton and B. O. Bengtsson. The barrier to genetic exchange between hybridising populations. *Heredity*, 56:357–376, Feb. 1986.

6. N. H. Barton. Multilocus Clines. *Evolution*, 37(3):454, May 1983.

7. G. Bhatia, N. Patterson, S. Sankararaman, and A. L. Price. Estimating and interpreting FST: the impact of rare variants. *Genome Research*, 23(9):1514–1521, Sept. 2013.

8. P. J. Bickel, N. Boley, J. B. Brown, H. Huang, and N. R. Zhang. Subsampling methods for genomic inference. *The Annals of Applied Statistics*, 4(4):1660–1697, Dec. 2010.

9. K. Bozek, J. Rangel, J. Arora, M. Tin, E. Crotteau, G. Loper, J. Fewell, and A. Mikheyev. Parallel genomic evolution of parasite tolerance in wild honey bee populations. *bioRxiv*, 2018.

10. R. Buggs. Empirical study of hybrid zone movement. *Heredity*, 99(3):301–312, 2007.

11. T. H. G. S. Consortium. Insights into social insects from the genome of the honeybee *Apis mellifera*. *Nature*, 444(7118):512–512, Nov. 2006.

12. R. Corbett-Detig and R. Nielsen. A Hidden Markov Model Approach for Simultaneously Estimating Local Ancestry and Admixture Time Using Next Generation Sequence Data in Samples of Arbitrary Ploidy. *PLoS Genetics*, 13(1):e1006529, Jan. 2017.

13. J. M. Cridland, S. R. Ramírez, C. A. Dean, A. Sciligo, and N. D. Tsutsui. Genome sequencing of museum specimens reveals rapid changes in the genetic composition of honey bees in California. *Genome Biology and Evolution*, 10(2):458–472, Jan. 2018.

14. J. M. Cridland, N. D. Tsutsui, and S. R. Ramírez. The complex demographic history and evolutionary origin of the western honey bee, *Apis mellifera*. *Genome Biology and Evolution*, 9(2):457–472, Feb. 2017.

15. M. Currat, M. Ruedi, R. J. Petit, and L. Excoffier. The hidden side of invasions: massive introgression by local genes. *Evolution*, 62(8):1908–1920, 2008.

16. L. C. Cwynar and G. M. MacDonald. Geographical Variation of Lodgepole Pine in Relation to Population History. *American Naturalist*, 129(3):463–469, Mar. 1987.

17. H. V. Daly and S. S. Balling. Identification of Africanized honeybees in the Western Hemisphere by discriminant analysis. *Journal of the Kansas Entomological Society*, 1978.

18. H. V. Daly, K. Hoelmer, and P. Gambino. Clinal geographic variation in feral honey bees in California, USA. *Apidologie*, 22(6):591–609, 1991.

19. R. G. Danka, R. L. Hellmich, T. E. Rinderer, and A. M. Collins. Diet-selection ecology of tropically and temperately adapted honey-bees. *Animal Behaviour*, 35(6):1858–1863, Dec. 1987.

20. R. G. Danka, T. E. Rinderer, R. L. Hellmich, and A. M. Collins. Comparative toxicities of four topically applied insecticides to Africanized and European honey bees (Hymenoptera: Apidae). *Journal of Economic Entomology*, 79(1):18–21, Feb. 1986.

21. A. R. De La Torre, T. Wang, B. Jaquish, and S. N. Aitken. Adaptation and exogenous selection in a picea glauca × picea engelmannii hybrid zone: implications for forest management under climate change. *New Phytologist*, 201(2):687–699, 2014.

22. L. Excoffier, M. Foll, and R. J. Petit. Genetic consequences of range expansions. *Annual Review of Ecology, Evolution, and Systematics*, 40(1):481–501, Dec. 2009.

23. J. H. Fewell and S. M. Bertram. Evidence for genetic variation in worker task performance by African and European honey bees. *Behavioral Ecology and Sociobiology*, 52(4):318–325, Sept. 2002.

24. B. M. Fitzpatrick, J. R. Johnson, D. K. Kump, J. J. Smith, S. R. Voss, and H. B. Shaffer. Rapid spread of invasive genes into a threatened native species. *Proceedings of the National Academy of Sciences USA*, 107(8):3606–3610, Feb. 2010.

25. T. P. Good, J. C. Ellis, C. A. Annett, and R. Pierotti. Bounded hybrid superiority in an avian hybrid zone: effects of mate, diet, and habitat choice. *Evolution*, 54(5):1774–1783, 2000.

26. D. Goulson, E. Nicholls, C. Botías, and E. L. Rotheray. Bee declines driven by combined stress from parasites, pesticides, and lack of flowers. *Science*, 347(6229):1255957–1255957, Mar. 2015.

27. K. E. Grinde, L. A. Brown, A. P. Reiner, T. A. Thornton, and S. R. Browning. Genome-wide significance thresholds for admixture mapping studies. *American Journal of Human Genetics*, 104(3):454–465, Mar. 2019.

28. J. Guerra, L. S. Goncalves, and D. De Jong. Africanized honey bees (Apis mellifera L.) are more efficient at removing worker brood artificially infested with the parasitic mite Varroa jacobsoni Oudemans than are Italian bees or Italian/Africanized hybrids. *Genetics and Molecular Biology*, 23(1):89–92, Mar. 2000.

29. E. Guzman-Novoa, R. Vandame, and M. E. Arechavaleta. Susceptibility of European and Africanized honey bees (Apis mellifera L.) to Varroa jacobsoni Oud. in Mexico. *Apidologie*, 30(2-3):173–182, 1999.

30. B. A. Harpur, C. F. Kent, D. Molodtsova, J. M. D. Lebon, A. S. Alqarni, A. A. Owayss, and A. Zayed. Population genomics of the honey bee reveals strong signatures of positive selection on worker traits. *Proceedings of the National Academy of Sciences USA*, 111(7):2614–2619, Feb. 2014.

31. J. F. Harrison, J. H. Fewell, K. E. Anderson, and G. M. Loper. Environmental physiology of the invasion of the Americas by Africanized honeybees. *Integrative and Comparative Biology*, 46(6):1110–1122, Oct. 2006.

32. R. J. Hijmans, S. E. Cameron, J. L. Parra, P. G. Jones, and A. Jarvis. Very high resolution interpolated climate surfaces for global land areas. *International Journal of Climatology*, 25(15):1965–1978, Dec. 2005.

33. J. K. Hill, C. D. Thomas, and D. S. Blakeley. Evolution of flight morphology in a butterfly that has recently expanded its geographic range. *Oecologia*, 121(2):165–170, Nov. 1999.

34. J. A. Hodgson, J. K. Pickrell, L. N. Pearson, E. E. Quillen, A. Prista, J. Rocha, H. Soodyall, M. D. Shriver, and G. H. Perry. Natural selection for the Duffy-null allele in the recently admixed people of Madagascar. *Proceedings. Biological sciences*, 281:20140930, Aug. 2014.

35. D. W. Huang, B. T. Sherman, and R. A. Lempicki. Systematic and integrative analysis of large gene lists using DAVID bioinformatics resources. *Nature Protocols*, 4(1):44–57, Jan. 2009.

36. M. B. Hufford, P. Lubinksy, T. Pyhäjärvi, M. T. Devengenzo, N. C. Ellstrand, and J. Ross-Ibarra. The genomic signature of crop-wild introgression in maize. *PLoS Genetics*, 9(5):e1003477, May 2013.

37. G. J. Hunt, G. V. Amdam, D. Schlipalius, C. Emore, N. Sardesai, C. E. Williams, O. Rueppell, E. Guzmán-Novoa, M. Arechavaleta-Velasco, S. Chandra, M. K. Fondrk, M. Beye, and R. E. Page. Behavioral genomics of honeybee foraging and nest defense. *Die Naturwissenschaften*, 94(4):247–267, Apr. 2007.

38. G. J. Hunt, E. Guzman-Novoa, M. K. Fondrk, and R. E. Page. Quantitative trait loci for honey bee stinging behavior and body size. *Genetics*, 148(3):1203–1213, Mar. 1998.

39. G. J. Hunt, E. Guzmán-Novoa, J. L. Uribe-Rubio, and D. Prieto-Merlos. Genotype–environment interactions in honeybee guarding behaviour. *Animal Behaviour*, 66(3):459–467, Sept. 2003.

40. J. C. Jones, A. Wallberg, M. J. Christmas, K. M. Kapheim, M. T. Webster, and N. Singh. Extreme differences in recombination rate between the genomes of a solitary and a social bee. *Molecular Biology and Evolution*, 36(10):2277–2291, May 2019.

41. S. M. Kadri, B. A. Harpur, R. O. Orsi, and A. Zayed. A variant reference data set for the Africanized honeybee, Apis mellifera. *Scientific Data*, 3:160097, Nov. 2016.

42. R. B. Kent. The introduction and diffusion of the African honeybee in South America. *Yearbook of the Association of Pacific Coast Geographers*, 50(1):21–43, 1988.

43. Y. Kono and J. R. Kohn. Range and frequency of Africanized honey bees in California (USA). *PLoS ONE*, 10(9):e0137407, Sept. 2015.

44. T. S. Korneliussen, A. Albrechtsen, and R. Nielsen. ANGSD: Analysis of Next Generation Sequencing Data. *BMC bioinformatics*, 15(1):356, Dec. 2014.

45. B. Langmead and S. L. Salzberg. Fast gapped-read alignment with Bowtie 2. *Nature methods*, 9(4):357–359, Mar. 2012.

46. W. Lin, J. McBroome, M. Rehman, and B. R. Johnson. Africanized bees extend their distribution in California. *PLoS ONE*, 13(1):e0190604, 2018.

47. J. C. Long. The genetic structure of admixed populations. *Genetics*, 127(2):417–428, Feb. 1991.

48. G. M. Loper, J. Fewell, D. R. Smith, W. S. Sheppard, and N. Schiff. Changes in the genetics of a population of feral honey bees (Apis mellifera L.) in S. Arizona after the impact of tracheal mites (Acarapis woodi), Varroa mites (Varroa jacobsoni) and Africanization. In R. Hoopingarner and L. Connor, editors, *Apiculture for the 21st Century*, pages 47–51. Wicwas, Cheshire, CT, 1999.

49. C. M. McDonnell, C. Alaux, H. Parrinello, J.-P. Desvignes, D. Crauser, E. Durbesson, D. Beslay, and Y. Le Conte. Ecto- and endoparasite induce similar chemical and brain neurogenomic responses in the honey bee (Apis mellifera). *BMC Ecology*, 13(1):1–15, Dec. 2013.

50. C. A. Medina-Flores, E. Guzman-Novoa, M. M. Hamiduzzaman, C. F. Aréchiga-Flores, and M. A. López-Carlos. Africanized honey bees (*Apis mellifera*) have low infestation levels of the mite Varroa destructor in different ecological regions in Mexico. *Genetics and Molecular Research*, 13(3):7282–7293, 2014.

51. J. Meisner and A. Albrechtsen. Inferring Population Structure and Admixture Proportions in Low-Depth NGS Data. *Genetics*, 210(2):719–731, Oct. 2018.

52. C. A. Miller, O. Hampton, C. Coarfa, and A. Milosavljevic. ReadDepth: A Parallel R Package for Detecting Copy Number Alterations from Short Sequencing Reads. *PLoS ONE*, 6(1):e16327, 2011.

53. G. Moretto and L. J. de Mello. Varroa jacobsoni infestation of adult Africanized and Italian honey bees (Apis mellifera) in mixed colonies in Brazil. *Genetics and Molecular Biology*, 22(3):321–323, Sept. 1999.

54. R. M. Nelson, A. Wallberg, Z. L. P. Simões, D. J. Lawson, and M. T. Webster. Genome-wide analysis of admixture and adaptation in the Africanized honeybee. *Molecular Ecology*, 26:3603–3617, Apr. 2017.

55. P. R. Oxley, M. Spivak, and B. P. Oldroyd. Six quantitative trait loci influence task thresholds for hygienic behaviour in honeybees (*Apis mellifera*). *Molecular Ecology*, 19(7):1452–1461, Apr. 2010.

56. B. L. Phillips, G. P. Brown, J. K. Webb, and R. Shine. Invasion and the evolution of speed in toads. *Nature*, 439(7078):803–803, Feb. 2006.

57. M. A. Pinto, W. L. Rubink, J. C. Patton, R. N. Coulson, and J. S. Johnston. Africanization in the United States: replacement of feral European honeybees (*Apis mellifera* L.) by an African hybrid swarm. *Genetics*, 170(4):1653–1665, Aug. 2005.

58. T. E. Rinderer, H. A. Sylvester, M. A. Brown, J. D. Villa, D. Pesante, and A. M. Collins. Field and simplified techniques for identifying Africanized and European honey bees. *Apidologie*, 17(1):13–48, 1986.

59. B. A. Rowan, D. Heavens, T. R. Feuerborn, A. J. Tock, I. R. Henderson, and D. Weigel. An ultra high-density Arabidopsis thaliana crossover map that refines the influences of structural variation and epigenetic features. *Genetics*, 213(3):771–787, Nov. 2019.

60. F. Ruttner. *Biogeography and Taxonomy of Honeybees.* Springer, Berlin, 1988.

61. S. S. Schneider, G. DeGrandi-Hoffman, and D. R. Smith. The African honey bee: Factors contributing to a successful biological invasion. *Annual Review Entomology*, 49(1):351–376, Dec. 2004.

62. W. S. Sheppard, T. E. Rinderer, J. A. Mazzoli, J. A. Stelzer, and H. Shimanuki. Gene flow between African- and European-derived honey bee populations in Argentina. *Nature*, 349(6312):782–784, Feb. 1991.

63. D. Siegmund and B. Yakir. *The Statistics of Gene Mapping.* Springer Science & Business Media, May 2007.

64. A. D. Simmons and C. D. Thomas. Changes in Dispersal during Species' Range Expansions. *American Naturalist*, 164(3):378–395, July 2015.

65. L. Skotte, T. S. Korneliussen, and A. Albrechtsen. Estimating individual admixture proportions from next generation sequencing data. *Genetics*, 195(3):693–702, Nov. 2013.

66. E. E. Southwick, D. W. Roubik, and J. M. Williams. Comparative energy balance in groups of Africanized and European honey bees: ecological implications. *Comparative Biochemistry and Physiology*, 97(1):1–7, 1990.

67. A. Spötter, P. Gupta, G. Nuernberg, N. Reinsch, and K. Bienefeld. Development of a 44K SNP assay focussing on the analysis of a varroa-specific defence behaviour in honey bees (*Apis mellifera carnica*). *Molecular Ecology Resources*, 12(2):323–332, Mar. 2012.

68. C. Surlis, J. C. Carolan, M. Coffey, and K. Kavanagh. Quantitative proteomics reveals divergent responses in Apis mellifera worker and drone pupae to parasitization by Varroa destructor. *Journal of Insect Physiology*, 107:291–301, May 2018.

69. J. M. Szymura and N. H. Barton. Genetic analysis of a hybrid zone between the fire-bellied toads, Bombina bombina and B. variegata, near Cracow in southern Poland. *Evolution*, 40(6):1141, Nov. 1986.

70. J. M. Szymura and N. H. Barton. The genetic structure of the hybrid zone between the fire-bellied toads Bombina bombina and B. variegata: Comparisons between transects and between loci. *Evolution*, 45(2):237, Mar. 1991.

71. H. Tavares, A. Whibley, D. L. Field, D. Bradley, M. Couchman, L. Copsey, J. Elleouet, M. Burrus, C. Andalo, M. Li, Q. Li, Y. Xue, A. B. Rebocho, N. H. Barton, and E. Coen. Selection and gene flow shape genomic islands that control floral guides. *Proceedings of the National Academy of Sciences USA*, 5:201801832, Oct. 2018.

72. S. A. Taylor, E. L. Larson, and R. G. Harrison. Hybrid zones: windows on climate change. *Trends in Ecology & Evolution*, 30(7):398–406, July 2015.

73. O. R. Taylor Jr and M. Spivak. Climatic limits of tropical African honeybees in the Americas. *Bee World*, 65(1):38–47, 1984.

74. K. C. Teeter, B. A. Payseur, L. W. Harris, M. A. Bakewell, L. M. Thibodeau, J. E. O'Brien, J. G. Krenz, M. A. Sans-Fuentes, M. W. Nachman, and P. K. Tucker. Genome-wide patterns of gene flow across a house mouse hybrid zone. *Genome Research*, 18(1):67–76, Jan. 2008.

75. T. Thornton, H. Tang, T. J. Hoffmann, H. M. Ochs-Balcom, B. J. Caan, and N. Risch. Estimating Kinship in Admixed Populations. *The American Journal of Human Genetics*, 91(1):122–138, July 2012.

76. J. M. Tsuruda, J. W. Harris, L. Bourgeois, R. G. Danka, and G. J. Hunt. High-resolution linkage analyses to identify genes that influence *Varroa* sensitive hygiene behavior in honey bees. *PLoS ONE*, 7(11):e48276, 2012.

77. USDA Agricultural Research Service. Spread of Africanized honey bees by year, by county, Mar. 2011.

78. R. Vandame, S. Morand, M. E. Colin, and L. P. Belzunces. Parasitism in the social bee Apis mellifera: quantifying costs and benefits of behavioral resistance to Varroa destructor mites. *Apidologie*, 33(5):433–445, 2002.

79. J. D. Villa, N. Koeniger, and T. E. Rinderer. Overwintering of Africanized, European, and hybrid honey bees in Germany. *Environmental Entomology*, 20(1):39–43, Feb. 1991.

80. A. Wallberg, I. Bunikis, O. V. Pettersson, M.-B. Mosbech, A. K. Childers, J. D. Evans, A. S. Mikheyev, H. M. Robertson, G. E. Robinson, and M. T. Webster. A hybrid de novo genome assembly of the honeybee, *Apis mellifera*, with chromosome-length scaffolds. *BMC Genomics*, 20(1):275, Dec. 2019.

81. A. Wallberg, F. Han, G. Wellhagen, B. Dahle, M. Kawata, N. Haddad, Z. L. P. Simões, M. H. Allsopp, I. Kandemir, P. De la Rúa, C. W. Pirk, and M. T. Webster. A worldwide survey of genome sequence variation provides insight into the evolutionary history of the honeybee *Apis mellifera*. *Nature Genetics*, 46(10):1081–1088, Aug. 2014.

82. S. Wang, S. Rohwer, K. Delmore, and D. E. Irwin. Cross-decades stability of an avian hybrid zone. *Journal of Evolutionary Biology*, 32(11):1242–1251, Nov. 2019.

83. C. W. Whitfield, S. K. Behura, S. H. Berlocher, A. G. Clark, J. S. Johnston, W. S. Sheppard, D. R. Smith, A. V. Suarez, D. Weaver, and N. D. Tsutsui. Thrice out of Africa: ancient and recent expansions of the honey bee, *Apis mellifera*. *Science*, 314(5799):642–645, Oct. 2006.

84. M. L. Winston. The biology and management of Africanized honey bees. *Annual Review of Entomology*, 37:173–193, 1992.

85. J. Woyke. Experiences with Apis mellifera adansonii in Brazil and in Poland. *Apiacta*, 1973.

Supporting information

S1 Table. Sample information. Geographic sampling information (population, location, date, whether collected by a feral nest), approximate sequencing coverage, global ancestry estimates and wing lengths for bees sequenced in this study and reference bees.

S2 Table. Cline model comparison. Model rankings between logistic cline fits for genome-wide African ancestry predicted by climate and distance variables.

	predictor	df.residual	deviance	dAIC	weight
1	Latitude	311	2.69	0.00	1.00
2	Mean temperature	311	3.63	93.60	0.00
3	Mean temperature of coldest quarter	311	5.25	208.60	0.00
4	Minimum temperature of coldest month	311	7.04	300.70	0.00
5	Distance to Sao Paulo	311	9.55	396.10	0.00
6	Annual precipitation	311	15.21	541.80	0.00

S3 Table. Ancestry outlier regions. Genome coordinates for outlier regions with high or low African (A) ancestry. Adjacent and near adjacent (within 10kb) ancestry windows meeting <10% FDR have been combined into contiguous regions and are labelled with the lowest FDR within the region. Note that shared high A outlier regions, by definition, will overlap high A South American and high A North American outlier regions, with bp and percent overlap listed. NA signifies not significant for that hybrid zone.

S4 Table. Ancestry outlier genes. List of genes overlapping ancestry outliers at 1%, 5%, and 10% FDR thresholds. Minimum FDR for each continent listed separately. NA signifies not significant for that hybrid zone.

S5 Table. Approximate QTL coordinates HAv3.1. Approximate coordinates (HAv3.1) for regions of the genome previously associated with defensive behaviors or *Varroa* tolerance.

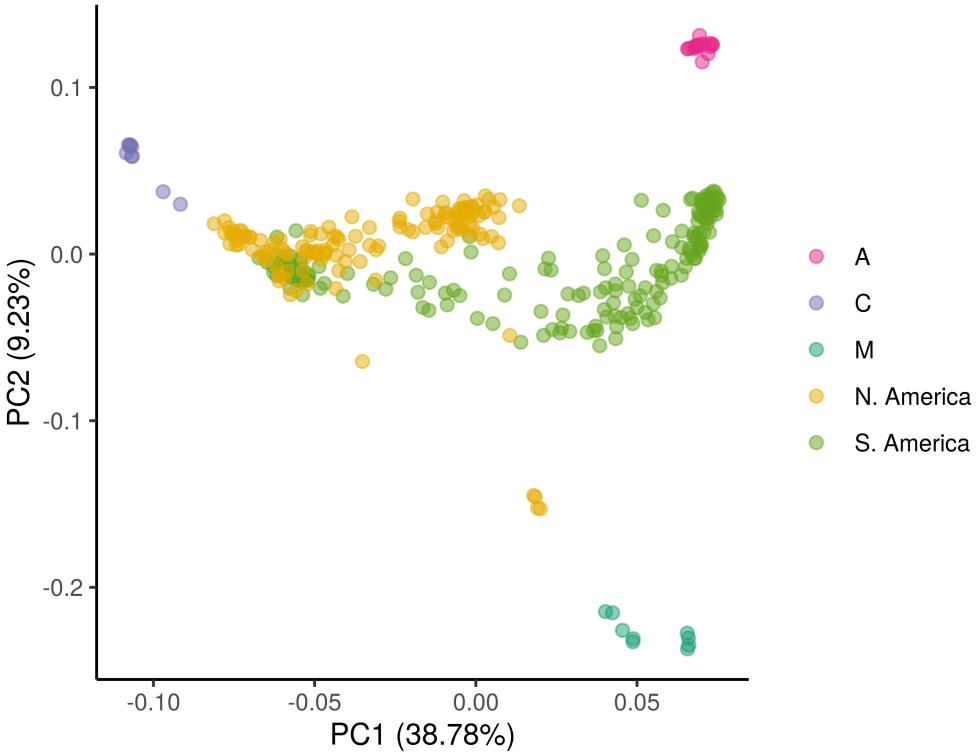

Fig 1. PCA. Principal components analysis generated in PCAngsd using genotype likelihoods from the same thinned set of 14,044 autosomal SNPs used in global admixture analysis. The major axes of diversity separate out C ancestry (PC1) and M ancestry (PC2). Consistent with 3-way admixture, all sampled bees from North and South America are intermediate on the PCA, in the triangle formed by reference panels for African (A), eastern European (C) and western European (M) honey bees.

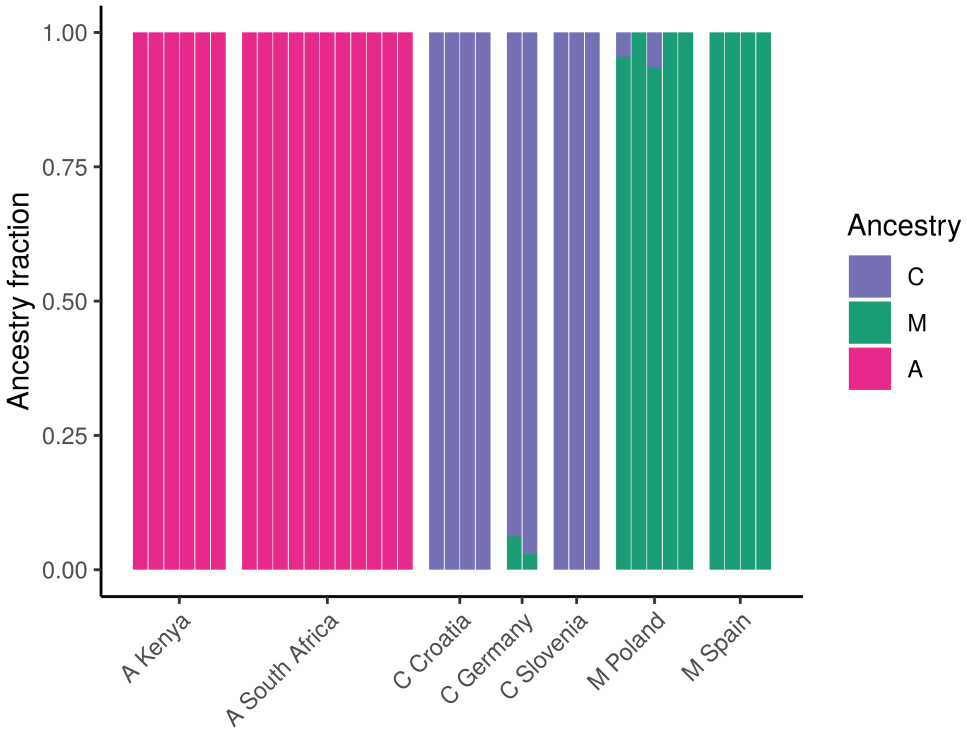

Fig 2. Ancestry in reference panels. Results of NGSAdmix global admixture analysis for reference populations from the combined analysis of all populations (K = 3). These results were used to assign the unlabelled ancestry components output by NGSAdmix to "A", "C", and "M" groups, based on a clear mapping to the three reference populations. We see a small amount of admixture between C and M within our reference populations, which is consistent with limited gene flow from secondary contact within Europe.

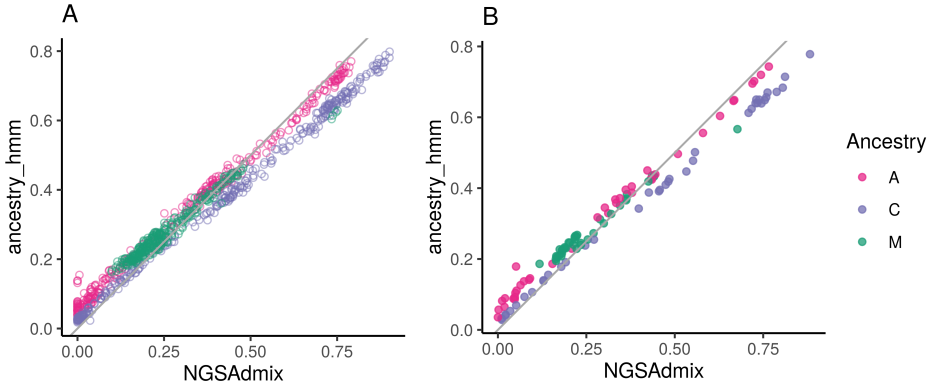

Fig 3. Comparison of local and global ancestry results. Comparison of the mean genome-wide ancestry inferred from NGSAdmix (x-axis) and ancestry_hmm (y-axis). Each individual bee (panel A) or population (panel B) is a point and the one-to-one line is drawn in gray. The mean for the HMM is calculated by marginalizing the posterior over all ancestry states and taking a mean across SNPs. The individual-level ancestry estimates between the two methods agree strongly (Pearson's correlation: 0.997 A, 0.999 C, 0.985 M), but the HMM infers slightly higher minor ancestry for bees with low admixture proportions. These two estimates are not entirely independent, as population mean ancestry proportions from NGSAdmix are used as a prior for the population-specific mixing proportions in ancestry_hmm, so panel B can also be interpreted as the prior and posterior of the local ancestry HMM for population-level admixture proportions.

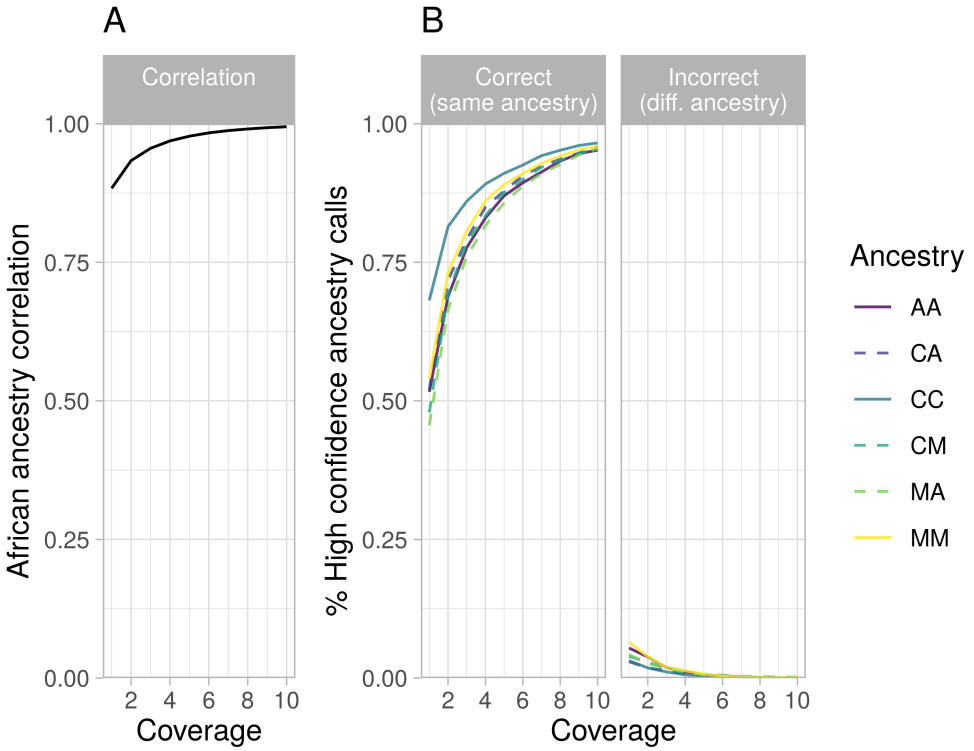

Fig 4. Power to call local ancestry. Results from a preliminary analysis of the power to call local ancestry accurately, used to inform target sequencing depth for this study. The x-axis shows the simulated mean depth of coverage (1-10x). In Fig A, the y-axis shows the correlation between high-coverage and low-coverage ancestry calls, while in Fig B the y-axis shows the proportion of high-confidence ancestry calls from high-coverage data that were replicated in an analysis of simulated low-coverage data. For this preliminary study, we used a published SNP set with data for A, C, and M reference populations [14] based on earlier versions of the honey bee genome (Amel4.5 [11]) and recombination map [81]. We enriched for ancestry-informativeness and thinned for LD (≥ 0.2 MAF in at least one reference population and $r^2 < 0.4$ within the A reference population), leaving 161k SNPs. First we ran ancestry_hmm [12] using called genotypes from a high-coverage admixed population with intermediate admixture proportions (Riverside 2014 (n=8): 40% C, 20% M, 40% A ancestry). We simulated lower coverage data from this same population by generating a binomial sample of n reads for each locus, based on the individual's genotype. To simulate realistic variance in coverage across the genome, n for each site and individual was generated from a negative binomial distribution with variance 3x the mean [52]. We additionally simulated a 1% sequencing error rate. Running local ancestry inference on the high coverage data, we inferred high confidence ancestry states for 81% of sites. First we calculated a point estimates for African ancestry ($p(AA) + 1/2(p(CA) + p(MA))$) at every site for each individual and used these estimates to calculate a correlation between the high coverage ancestry calls and low coverage ancestry calls (Fig A). Then we calculated the percent of high confidence calls that were replicated with high confidence (≥ 0.8 posterior) in the low coverage data for the same ancestry state ("correct") or a different ancestry state ("incorrect") (Fig B). Call to the HMM for simulated low-coverage data: ancestry_hmm -e 3e-3 -a 3 0.4 0.2 0.4 -p 0 100000 0.4 -p 1 -100 0.2 -p 2 -60 0.4 –tmax 150 –tmin 2 –ne 670000. For original high coverage data we used genotype calls rather than read counts (-g) and a lower error rate (-e 1e-3).

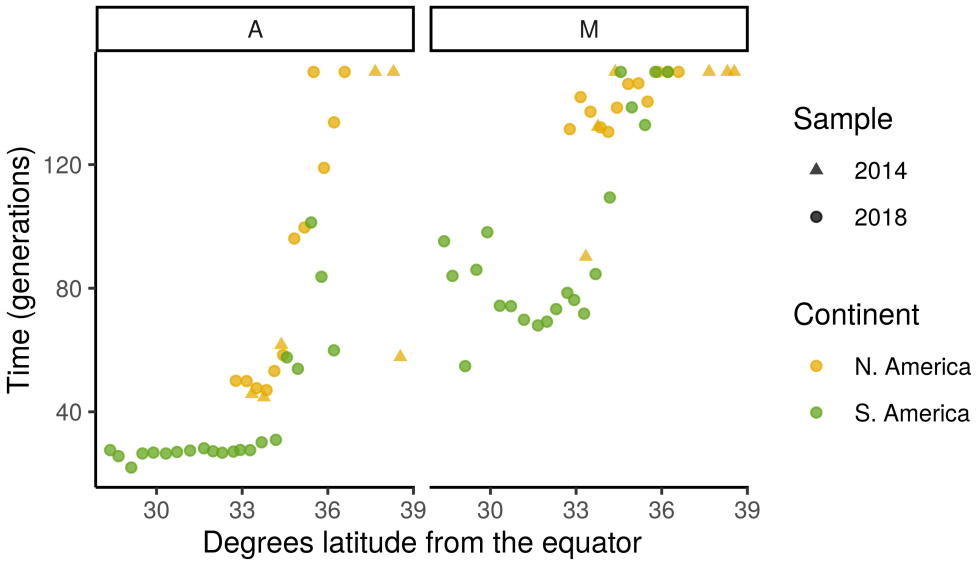

Fig 5. Estimated generations post-admixture. Inferred timing of migration pulses from A ancestry (left) and M ancestry (right). Each population's admixture timing is estimated separately, during local ancestry inference (ancestry_hmm), and results are plotted across latitude. We allowed a range of 2-150 generations, so the highest time estimates are truncated at 150 generations. Admixture with African (A) ancestry began in 1956, 62 years before sampling in 2018. We have little prior information about the timing of M into C admixture, which likely varies across the Americas, but in general should pre-date Africanization. The number of generations per year for feral honey bee populations is uncertain.

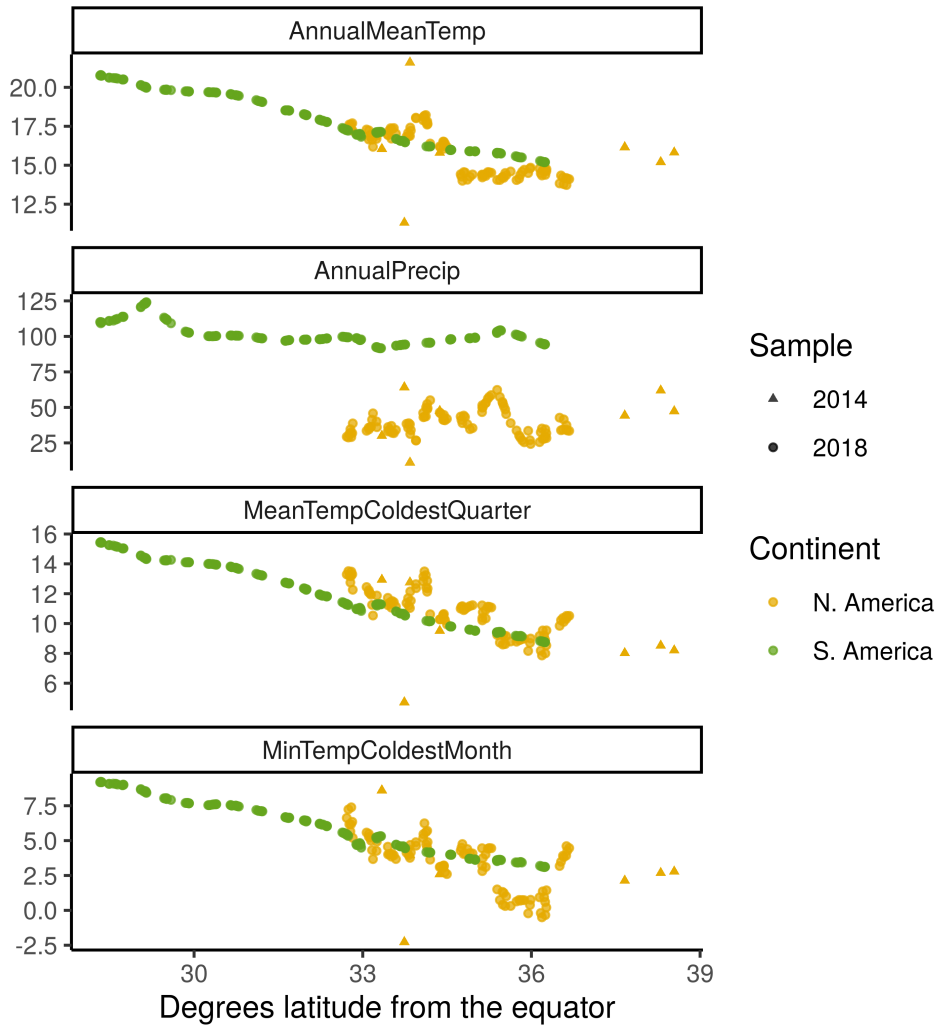

Fig 6. Climate variables across latitude. Bioclim climate variables for all sample sites plotted against latitude: (A) Mean annual temperature (B) Mean annual precipitation (C) Mean temperature coldest quarter (D) Minimum temperature coldest month. Two adjacent climate outliers in the N. American sample can be seen in the top two panels and represent bees from an inland desert (hot and dry) and a high altitude sampling site (cold and wet) at similar latitudes in Riverside County, CA. Bees from this same high altitude site are also outliers in the bottom two panels, having the coldest mean and minimum winter temperatures of all sites.

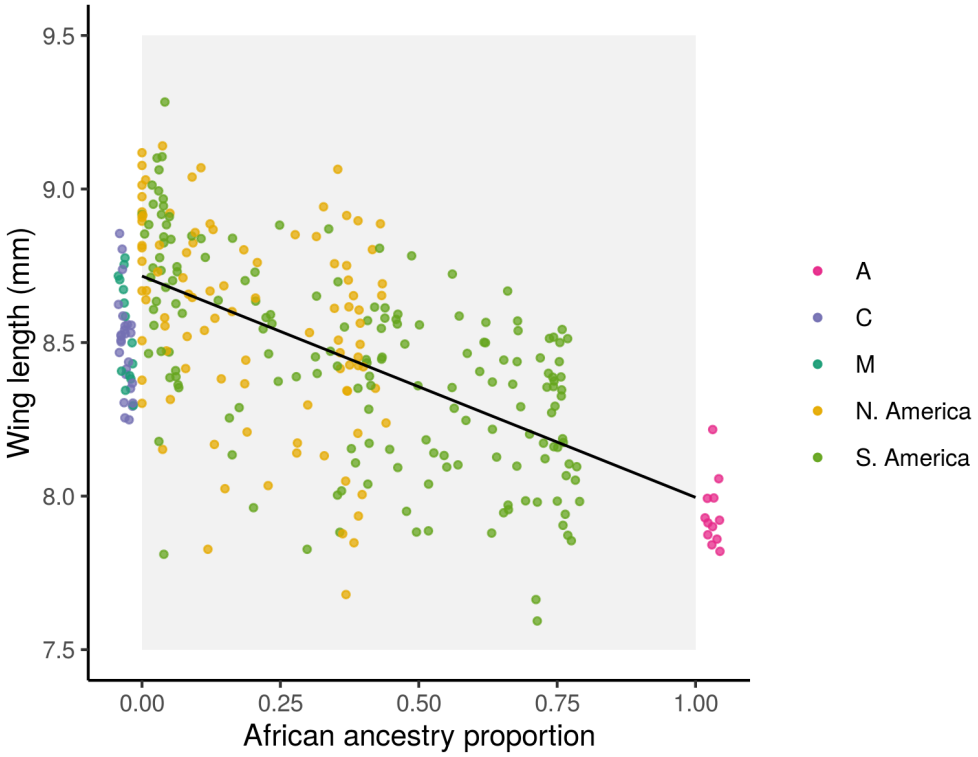

Fig 7. Wing length predicted by African ancestry. Individual honey bees are represented as points, with wing lengths plotted along the x-axis and genonewide African ancestry proportions (NGSAdmix results) along the y-axis. We draw the best-fit regression line (slope = -0.72 mm, $F(1, 267) = 119$, $P = 3.65 \times 10^{-23}$, $R^2 = 0.31$, $n = 269$). We also include wing lengths for European (C, M) and African (A) reference bees from the Oberursel Collection, which we assume have none or full A ancestry. These reference bees are plotted slightly outside the range [0,1] and with jitter to facilitate viewing individual points that would otherwise all cluster on the boundaries.

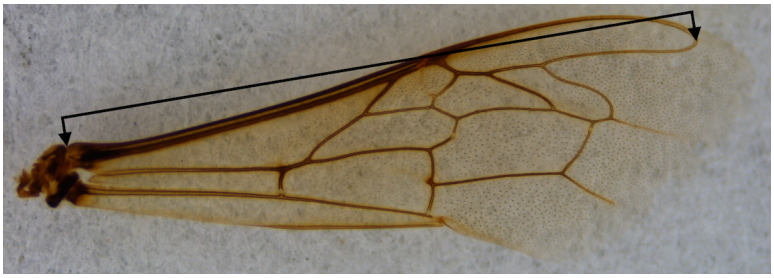

Fig 8. Wing length analysis. Fore wing image cropped and annotated to show length measurement taken. A full length to the tip of the wing is the standard measurement, but we use this alternative because many of our samples have significant wing tatter.

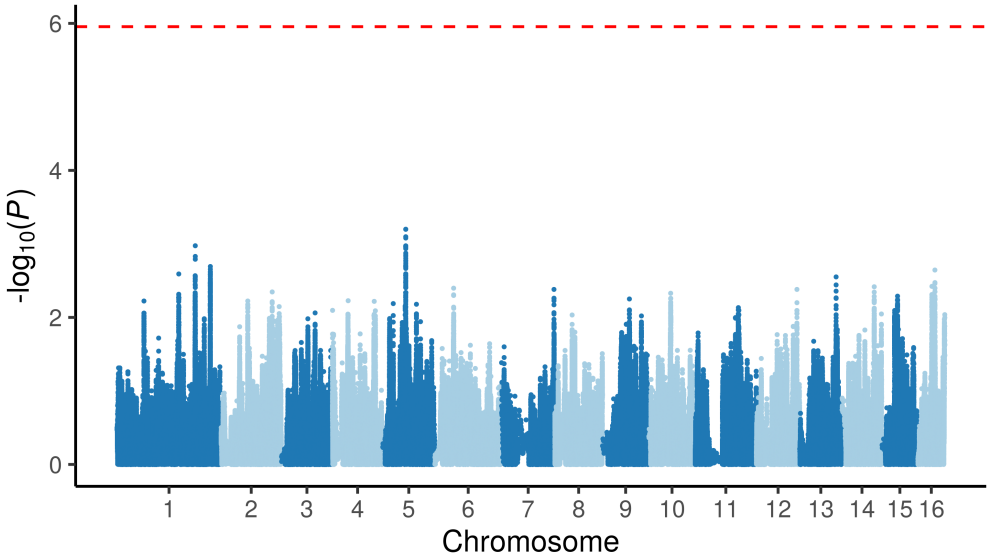

Fig 9. Admixture mapping analysis. We plot the p-value for each SNP across the genome, based on independent tests of association between African ancestry at that SNP and wing length. The red dashed line marks the genome-wide significance threshold for a family-wise error rate of 0.05, using a two-tailed test. In admixture mapping, SNPs are correlated, and the number of independent statistical tests depends on the number of generations recombination has had to break up ancestry blocks. Here we use an analytical approximation for the significance threshold based on 47.65 generations of admixture (population median estimate).

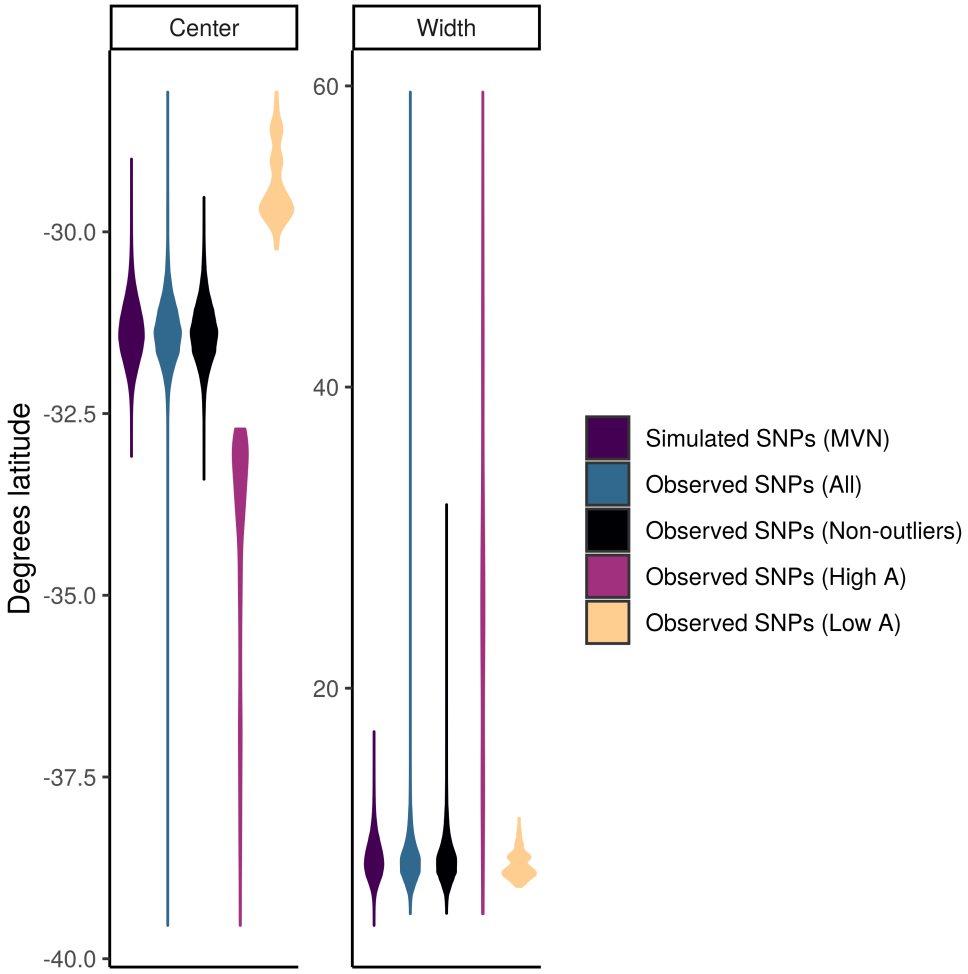

Fig 10. Distribution of ancestry clines in S. America across SNPs. A logistic cline model was fit to observed and simulated population ancestry frequencies across latitude for S. America. Estimated cline parameters, center and width ($w = |4/b|$), are presented as violin plots. Units for both cline center and width are degrees latitude. We additionally partition observed SNPs by outlier and non-outlier status, set by 10% FDR for high or low African ancestry in South America. Individual SNP clines were only fit in South America, where we observed the full cline.

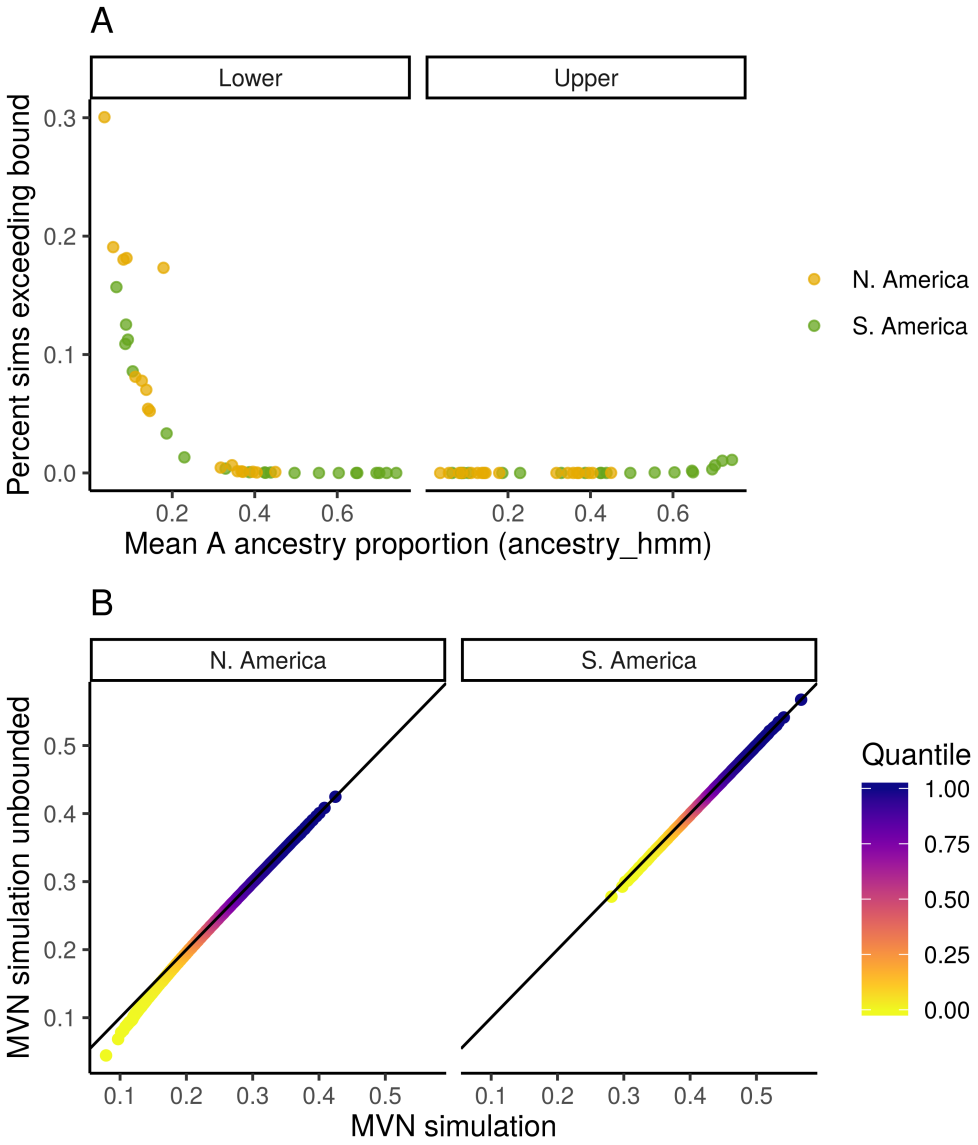

Fig 11. Effect of truncating MVN simulated ancestry frequencies. (A) Percent of simulated population A-ancestry frequencies exceeding lower (left) and upper (right) bounds, and thus truncated to [0,1] range. Each population is a point and the populations most affected by truncation are low-A ancestry populations with mean A-ancestry proportions close to the bound at 0. (B) QQ-plot comparing the quantiles for mean A ancestry before and after truncation in N. America (left) and S. America (right). The distribution of mean African ancestry is mostly unaffected by restricting simulated population A ancestry frequencies to the [0,1] range, but truncation does reduce model predictions of very low A-ancestry frequencies in N. America, where mean A ancestry is already low.

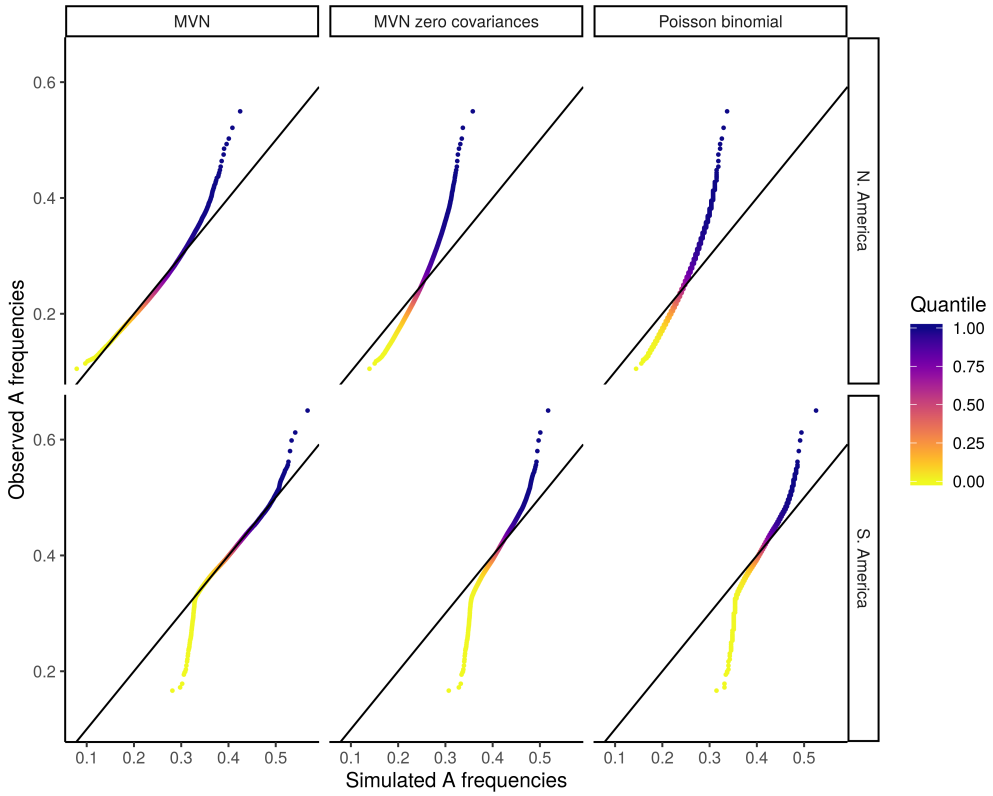

Fig 12. Simulated vs. observed African ancestry quantiles. QQ-plots comparing observed quantiles for mean African ancestry in North America (top) and South America (bottom) to the quantiles generated by three simulated distributions (left-to-right): MVN, MVN with zero covariances, and Poisson binomial model. Only the MVN model, allowing for covariances between populations, matches the bulk of the observed distribution.

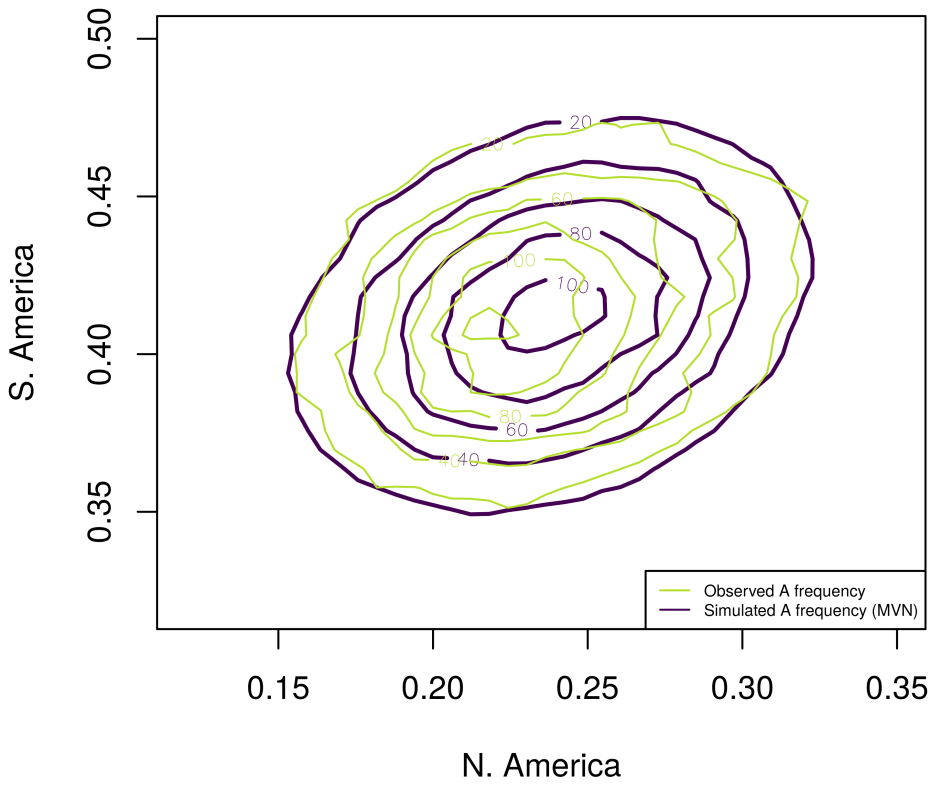

Fig 13. Overlay of 2D density plot for observed A ancestry frequencies in N. and S. America compared to simulated A ancestry frequencies under a multivariate-normal model.

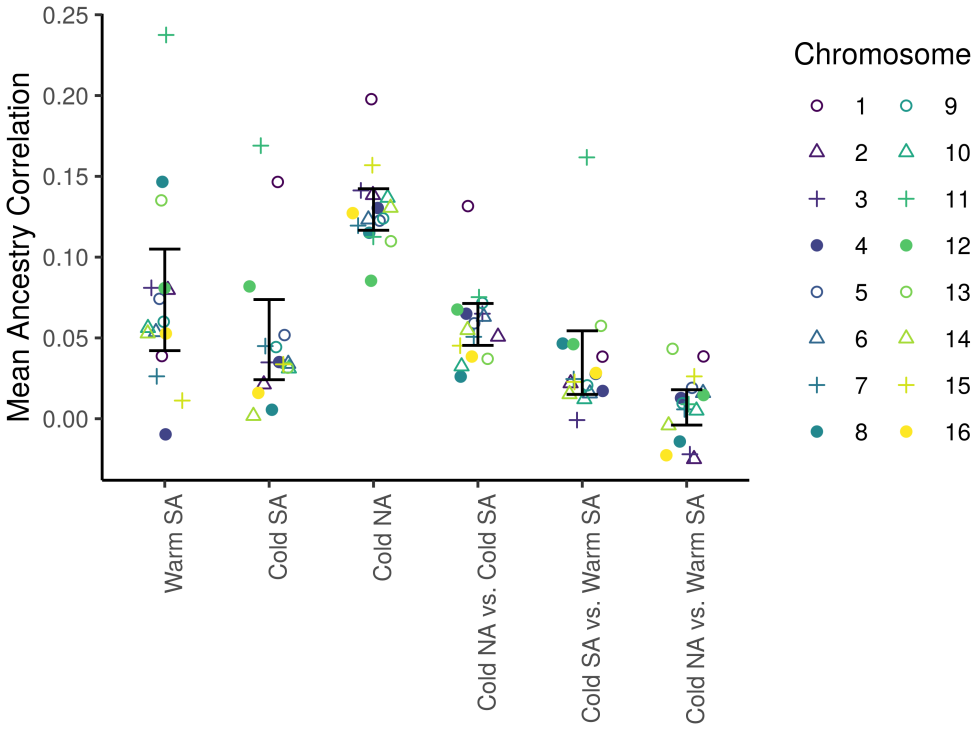

Fig 14. Mean ancestry correlation by chromosome across populations. Mean covariances (K matrices) are calculated separately for each chromosome, using the genome-wide mean ancestry, and then correlations are summarised by taking the mean for each type of population comparison, within and between continents and climatic regions. Additionally, error bars show the normal-approximated 95% confidence intervals around the mean. We divided populations in South America into two climatic regions based on having greater than ('warm') or less than ('cold') 50% mean African ancestry. All North American samples come from the 'cold' low-A side of the cline. On average across chromosomes, cold South American populations share higher ancestry correlations with cold North American populations than geographically closer warm South American populations (0.024: $CI_{95}[0.002, .045]$, P = .035, Paired 2-sided t-test). Two chromosomes harbor large outlier regions consistent with their elevated correlations shown here: Chromosome one has a large cluster of loci with high A ancestry in North and South America while chromosome 11 has a wide region of low A ancestry exclusive to South America. The results do not significantly differ if these two outlier chromosomes are both removed from the analysis (0.027: $CI_{95}[0.012, 0.041]$, P = 0.002, Paired 2-sided t-test).

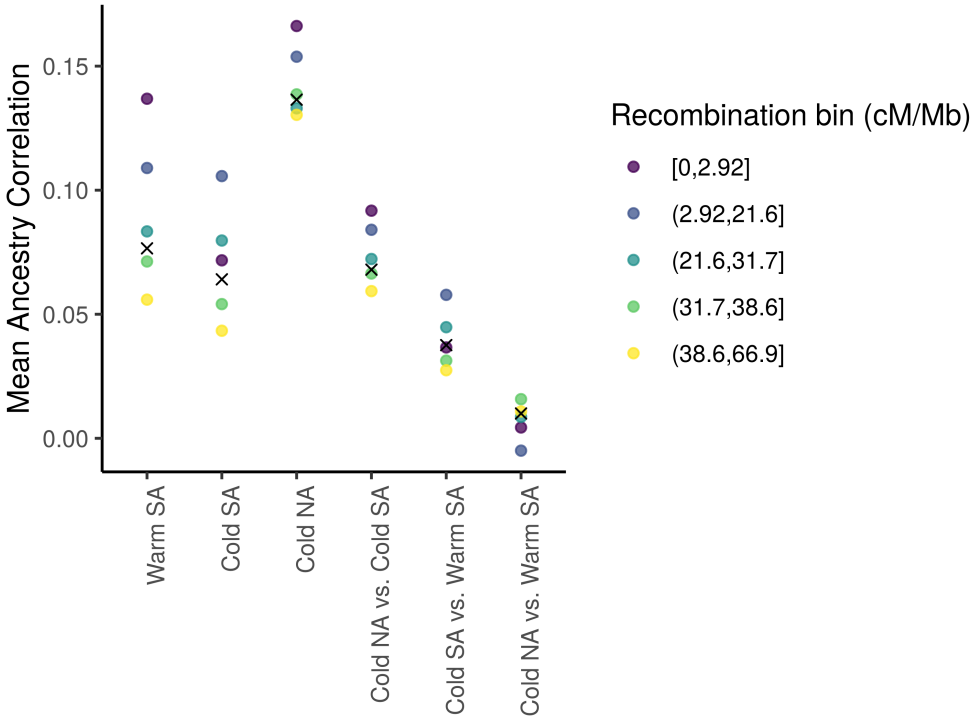

Fig 15. Mean correlation for population pairs by recombination rate. Mean ancestry and covariances (K matrices) are calculated separately for each of 5 recombination quintiles, then correlations are summarised by taking the mean for each type of population comparison, within and between continents and climatic regions. The genomewide mean is additionally shown as an X. We divided populations in South America into two climatic regions based on having greater than ('warm') or less than ('cold') 50% mean African ancestry. All North American samples come from the 'cold' low-A side of the cline. We tested whether cold South American populations share higher or lower ancestry correlations with cold North American populations than geographically closer warm South American populations. On average across recombination bins, we find that in this case ancestry correlations are higher for the more climatically similar, but geographically distant pairs (0.035: $CI_{95}[0.021, .050]$, P = .003, Paired 2-sided t-test)

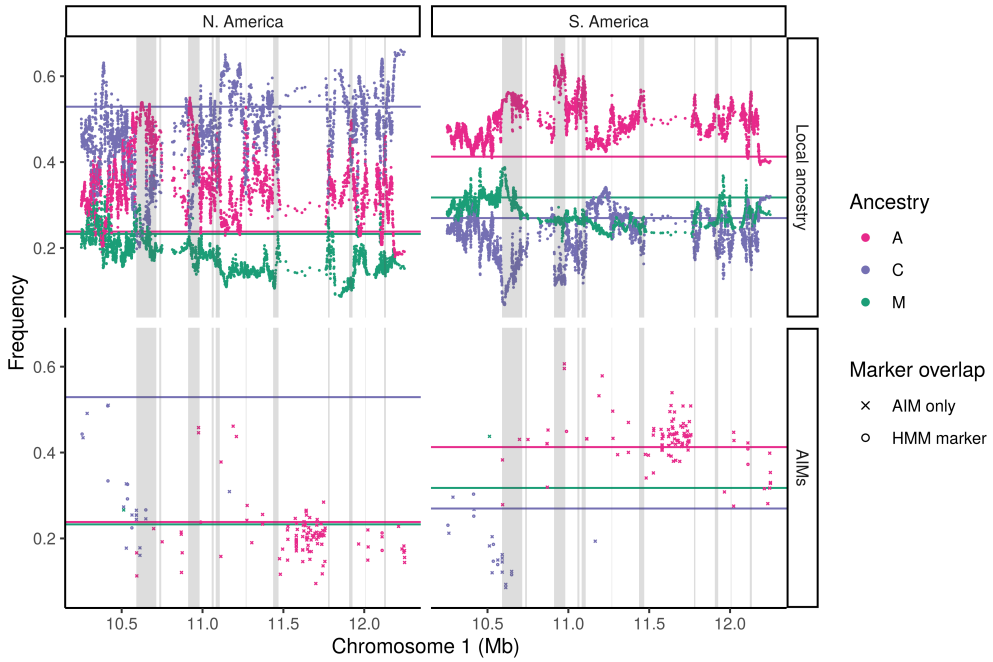

Fig 16. Ancestry and AIM frequencies for high shared A outliers on chr1. Zoomed-in view of the region on chromosome 1 with a cluster of high African ancestry peaks in both North America (left) and South America (right), with shared outliers meeting a 10% FDR for high African ancestry on both continents shaded in grey. (Top) African (A), western European (M) and eastern European (C) local ancestry estimates at each HMM marker. (Bottom) Mean frequency of ancestry informative markers AIMs (see methods), most of which were not included in the ancestry_hmm inference ('AIM only') due to LD thinning.

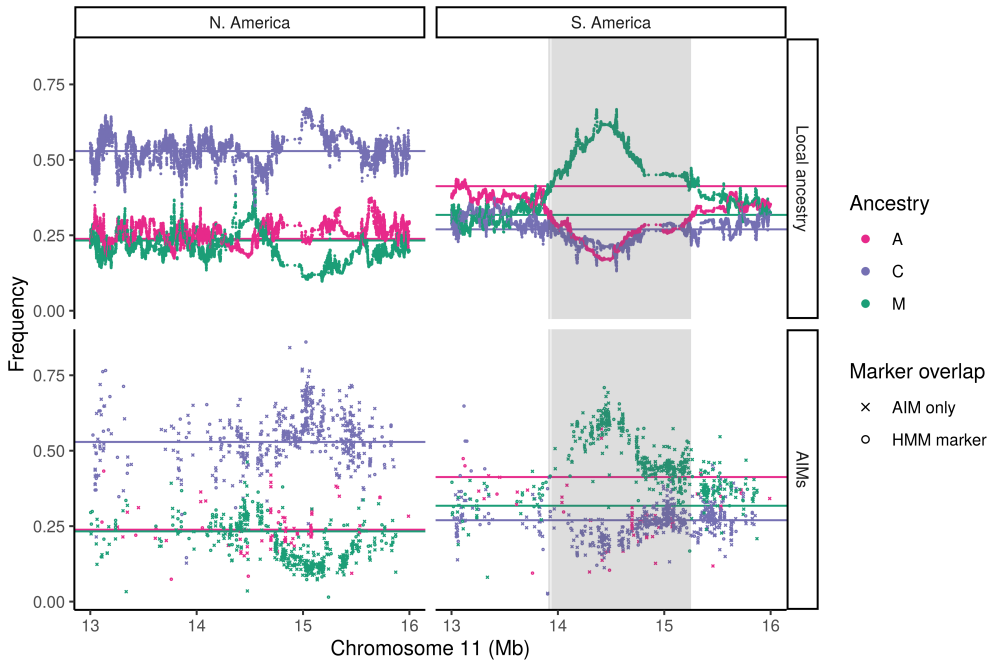

Fig 17. Ancestry and AIM frequencies for low A outlier region on chr11. Zoomed-in view of the 1.4Mb region on chromosome 11 with high western European ancestry (M) in South America (right) but not in North America (left), with the outlier region meeting 10% FDR highlighted in grey. (Top) African (A), western European (M) and eastern European (C) local ancestry estimates at each HMM marker. (Bottom) Mean frequency of ancestry informative markers AIMs (see methods), most of which were not included in the ancestry_hmm inference ('AIM only') due to LD thinning.

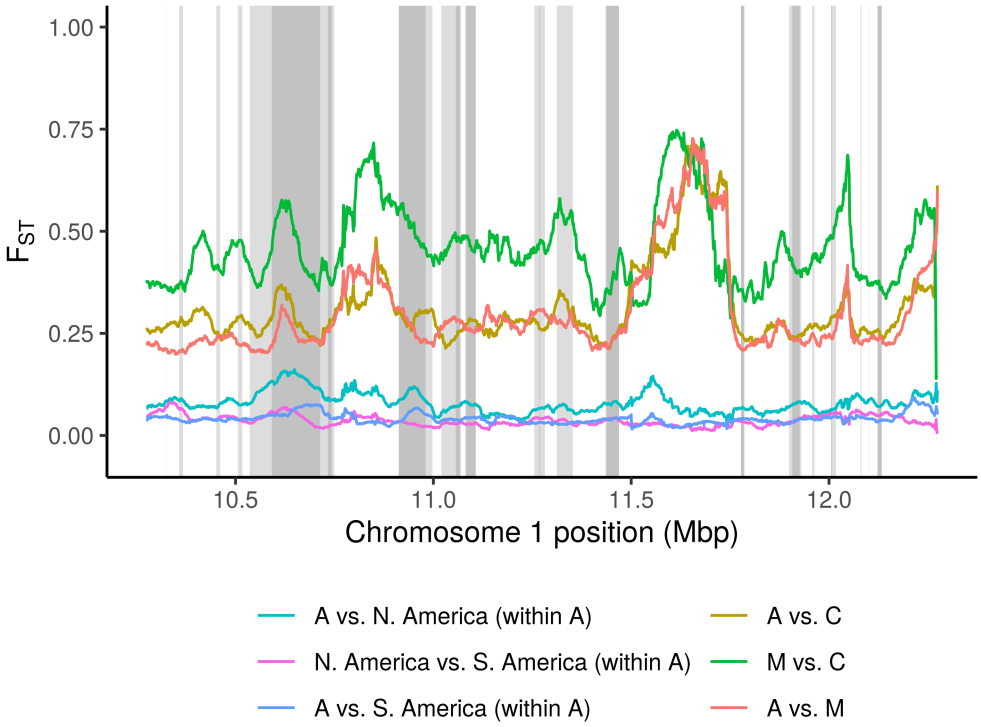

Fig 18. Differentiation across shared high A outliers on chr1. F_{ST} across the region on chromosome 1 with shared high African ancestry outliers. Outlier regions meeting a 10% FDR in both hybrid zones are highlighted in darker grey, while those meeting a 10% FDR in only one hybrid zone are highlighted in lighter grey. Per-SNP F_{ST} is averaged within sliding 50kb windows. In addition to the three ancestry reference panels (A, C, & M), we include contrasts for the subset of individuals in each hybrid zone with high-confidence homozygous A ancestry.

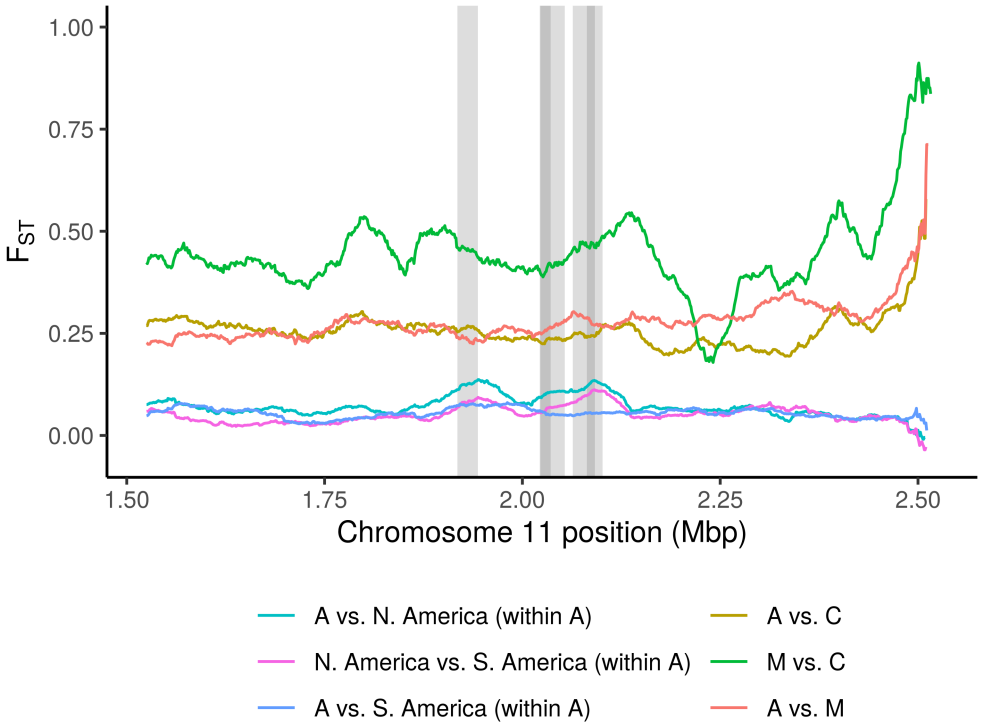

Fig 19. Differentiation across shared high A outliers on chr11. F_{ST} across the region on chromosome 11 with shared high African ancestry outliers. Outlier regions meeting a 10% FDR in both hybrid zones are highlighted in darker grey, while those meeting a 10% FDR in only one hybrid zone are highlighted in lighter grey. Per-SNP F_{ST} is averaged within sliding 50kb windows. In addition to the three ancestry reference panels (A, C, & M), we include contrasts for the subset of individuals in each hybrid zone with high-confidence homozygous A ancestry.

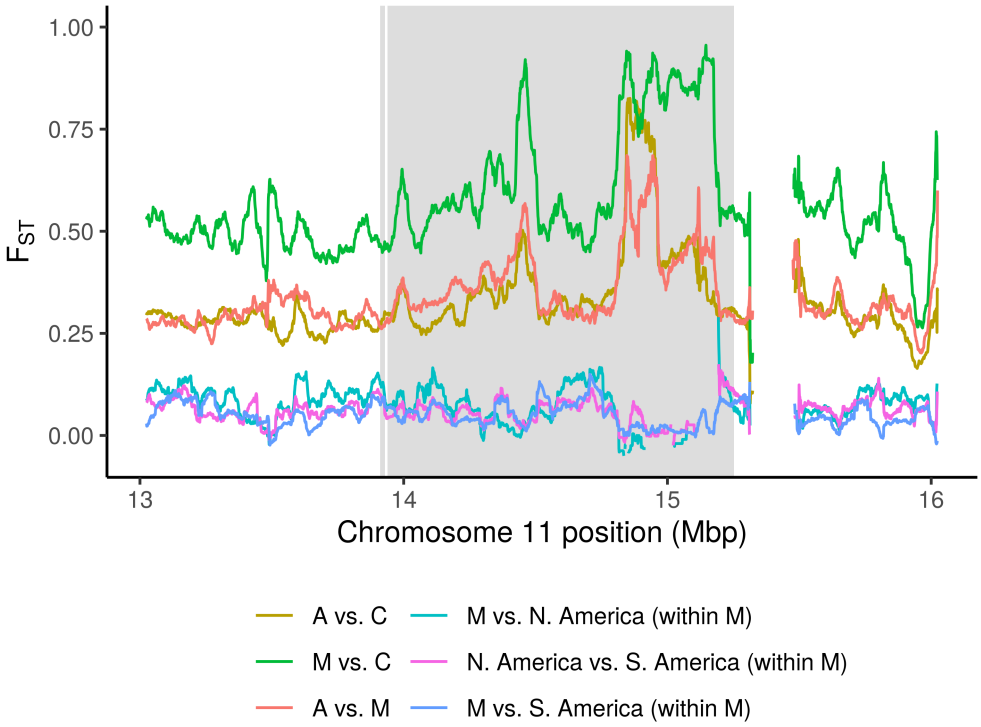

Fig 20. Differentiation across low A outlier region on chr11. F_{ST} across the 1.4Mb region on chromosome 11 with high western European ancestry (M) in South America but not in North America (left), with the outlier region meeting 10% FDR highlighted in grey. Per-SNP F_{ST} is averaged within sliding 50kb windows. In addition to the three ancestry reference panels (A, C, & M), we include contrasts for the subset of individuals in each hybrid zone with high-confidence homozygous M ancestry. Windows are dropped if fewer than 10 SNPs have 2 individuals with data, which produces gaps in the contrasts with N. American M ancestry because this hybrid zone does not have elevated M ancestry in this region and at many SNPs very few individuals have high-confidence homozygous M ancestry. Top peaks in M vs. C, M vs. A, and C vs. A contrasts seen within this region reach the 99.5, 98.0, and 99.8 percentiles (respectively) for 50kb windows genome-wide.

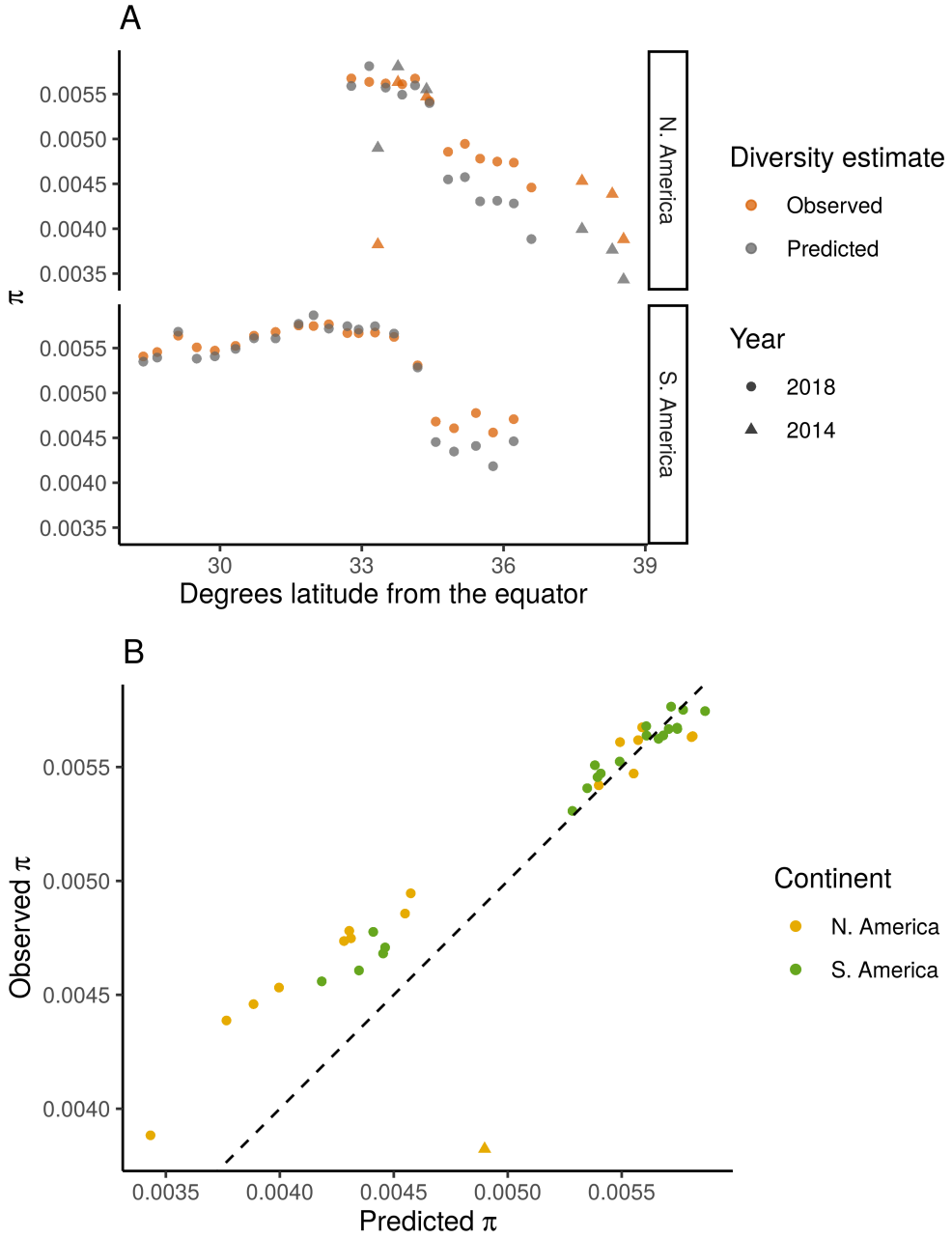

Fig 21. Comparison of observed and predicted diversity. A. Observed and predicted allelic diversity (π) for each population across latitude. To predict π for a specific population, we calculated the expected allele frequency based on a mixture of A, C, and M reference population allele frequencies, weighted by the population's estimated admixture fractions of these three ancestries. B. Plot of predicted vs. observed π for each population for direct comparison to the 1-to-1 line (dashed). Avalon (California 2014, marked as a triangle) is a clear outlier, with low diversity for its admixture fraction.